Establishment of a severe dengue disease murine model for preclinical CD8+ T cell targeting vaccine trials

Alice Hou

Department of Human Genetics
McGill University, Montreal

October 2024

A thesis submitted to McGill University in partial fulfilment of the requirements of the degree of Master of Science

Abstract

Dengue fever, a mosquito-borne disease, is responsible for approximately 390 million infections and 20,000 deaths worldwide each year. Since 2018, *Aedes* genus mosquitos, which transmit the dengue virus (DENV1-DENV4), have become locally established in Canada, increasing the risk for local dengue transmissions. A primary infection with one dengue strain does not provide long-term cross-protection against the other three strains, and a secondary infection with a different strain associates with an increased risk of severe dengue due to a phenomenon known as antibody-dependent enhancement (ADE). The goal of this project is to utilize genetically modified mice, in combination with the administration of anti-flavivirus antibodies as immunogens, to recapitulate key features of dengue fever. Establishing this murine model in the lab will provide a valuable platform for testing a novel CD8-targeting mRNA vaccine. We characterized the disease phenotype of type-I interferon alpha/beta receptor (IFNAR1) knockout mice following infection with a mouse-adapted dengue strain (D220). IFNAR1-/- mice that received anti-flavivirus antibodies prior to infection exhibited more severe clinical outcomes compared to both non-ADE and C57BL/6 resistant mice. Notably, vascular leakage, which is a symptom of severe dengue fever in human, was observed in IFNAR1-/- ADE mice during the acute phase of infection. Additionally, the viral load in IFNAR1-/- ADE mice was elevated compared to uninfected mice, with viral transcripts detected in organ samples. Furthermore, the infection elicited a robust CD8+ T cell response, including the shift of phenotype from naïve T cells to effector T cells and the secretion of IFNγ cytokines. Importantly, we have identified an indicator for dengue-experienced CD8+ T cells. These results suggest that severe dengue fever can be replicated in mice and highlight the crucial role of CD8+ T cells in host defense against DENV, providing a valuable resource for testing new preventive measures against severe dengue disease.

Résumé

La dengue, une maladie transmise par les moustiques, est responsable d'environ 390 million d'infections et de 20 000 décès dans le monde chaque année. Depuis 2018, les moustiques du genre Aedes, qui transmettent le virus de la dengue (DENV1-DENV4), se sont établis localement au Canada, augmentant le risque de transmission locale de la dengue. Une infection primaire avec une souche de dengue ne fournit pas de protection croisée à long terme contre les trois autres souches, et une infection secondaire avec une souche différente est associée à un risque accru de dengue sévère en raison d'un phénomène connu sous le nom de renforcement dépendant des anticorps (ADE). L'objectif de ce projet est d'utiliser des souris génétiquement modifiées, en combinaison avec l'administration d'anticorps anti-flavivirus comme immunogènes, pour récapituler les principales caractéristiques de la manifestation de la dengue. L'établissement de ce modèle murin en laboratoire fournira une plate-forme précieuse pour tester un nouveau vaccin ARNm ciblant les CD8. Nous avons caractérisé le phénotype de la maladie chez des souris knock-out pour le récepteur de l'interféron alpha/beta de type I (IFNAR1) après une infection par une souche de dengue adaptée à la souris (D220). Les souris IFNAR1-/- qui ont reçu des anticorps anti-flavivirus avant l'infection ont présenté des résultats cliniques plus graves que les souris non-ADE et les souris résistantes C57BL/6. Notamment, une fuite vasculaire, symptôme d'une dengue sévère chez l'homme, a été observée chez les souris IFNAR1-/- ADE pendant la phase aiguë de l'infection. En outre, la charge virale chez les souris IFNAR1-/- ADE était élevée par rapport aux souris non infectées, et des transcrits viraux ont été détectés dans des échantillons d'organes. En outre, l'infection a provoqué une réponse robuste des cellules T CD8+, y compris le changement de phénotype des cellules T naïves en cellules T effectrices et la sécrétion de cytokines IFNγ. Il est important de noter que nous avons identifié un indicateur pour les cellules T CD8+ expérimentées par la dengue. Ces résultats suggèrent que la dengue sévère peut être reproduite chez la souris et soulignent le rôle

crucial des cellules T CD8+ dans la défense de l'hôte contre le DENV, fournissant une ressource précieuse pour tester de nouvelles mesures préventives contre la dengue sévère.

Table of Contents

List of Abbreviations

ADCC: antibody dependent cellular cytotoxicity

ADE: antibody-dependent enhancement

APC: antigen presenting cell

C: capsid protein

Ct: cycle threshold

CDC: Centers for Disease Control and Prevention

CMC: carboxymethylcellulose

DENV: dengue virus

DHF: dengue hemorrhagic fever

DMEM: Dulbecco's Modified Eagle Medium

DSS: dengue shock syndrome

E: envelope protein

EDTA: ethylenediaminetetraacetic acid

FBS: fetal bovine serum

FFU: focus forming units

FMO: fluorescence minus one

IFN-γ: interferon gamma

IFNAR1: type-I interferon alpha/beta receptor

IgG: Immunoglobulin G

IL: interleukin

ISG: interferon-stimulated genes

JAK-STAT: Janus kinase/signal transducer and activator of transcription

JEV: Japanese encephalitis viruses

LCMV: lymphocytic choriomeningitis virus

M: membrane protein

MCP-1: monocyte chemoattractant protein 1

MDA5: melanoma differentiation-associated protein 5

MHC: major histocompatibility complex

MOI: multiplicity of infection

NS: non-structural proteins

OD: optical density

OVA: ovalbumin

PAMP: pathogen-associated molecular pattern

PBMC: peripheral blood mononuclear cell

PBS: phosphate buffered saline

PFU: plaque forming units

PRR: pathogen-recognizing receptors

RIG-1: retinoic acid-inducible gene I

RPMI: Roswell Park Memorial Institute

STING: stimulator of the interferon gene

TCR: T cell receptor

Th1: T helper 1

TLR: Toll-like receptor

TNFα: tumor necrosis factor alpha

TPB: tryptose phosphate broth

WHO: World Health Organization

WNV: West Nile virus

YFV: yellow fever virus

List of Figures

Acknowledgements

First and foremost, I extend my deepest gratitude to Dr. Silvia Vidal for accepting me into her lab during my final year of undergraduate studies. This opportunity to work alongside her lab members and researchers has been invaluable in my personal and academic development. I am especially thankful to her for allowing a young student, passionate about mouse models and disease manifestation, to begin exploring this field.

I would also like to express my sincere thanks to Nathan Markarian, an alumnus of the lab, who has been a mentor to me from the very first day. He patiently taught me everything, from laboratory techniques to scientific writing, and we have stayed in touch ever since. I wish him all the best in his future endeavors. I am equally grateful to Benoit Charbonneau and Patricia D'Arcy for their immense assistance with training me to conduct *in vivo* mouse infection experiments and necropsies, which were critical to the progress of my work.

My supervisory committee members — Dr. Jorg Fritz, Dr. Erwin Schurr, and Dr. Brian Ward — deserve my heartfelt thanks for their invaluable guidance and support throughout my research. I have greatly benefited from their insights and feedback.

I also want to acknowledge the sacrifice of the mice used in this project, as their contribution is fundamental to advancing scientific knowledge. Their sacrifice reminds me how carefully I must treat these precious samples and the respect I must uphold in my work. My friends and colleagues, now graduated and spread throughout the world, and those diligently working on the third floor of Bellini building, have provided laughter and friendship.

To my family, who have always believed in me and supported me in every way, I hope you can be proud of me for now being able to live healthily and share happy moments together. Finally, I would like to thank myself for growing into an individual of integrity, resilience, and dedication to lifelong learning. I never believed I could make it—until I did.

Format of the Thesis

Traditional Format

Contribution of Authors

Dr. Silvia Vidal supervised this project and provided mentorship throughout.

Nathan Markarian taught me essential laboratory techniques, including cell culturing, viral propagation, RNA extraction, PCR, and viral titration.

Benoit Charbonneau assisted with experiment planning and ordering materials.

Patricia D'Arcy managed the mouse colonies and supported me during mouse infections and necropsies.

Charlotte Fouquet helped maintain the cell cultures.

Dr. Jorg Fritz's lab provided training and guidance on flow cytometry.

My personal contributions included setting up mouse infections and monitoring them, tittering the virus, processing all sample, and conducting downstream analyses.

Chapter I: introduction and literature review

Clinical and Biological Context

Dengue is classified by the World Health Organization (WHO) as one of the neglected tropical diseases, characterized by features such as 1) association with poverty, 2) prevalence in tropical and subtropical regions, 3) high morbidity but low mortality, and 4) the absence of specific treatments [1]. Dengue is gaining public health attention due to the growing frequency and magnitude of outbreaks worldwide, leading to an estimate of over 390 million infections, including 294 million inapparent cases, 96 million apparent cases, and 20,000 deaths globally each year [2, 3]. This poses great threat in public health, especially due to the increased risk of severe dengue associated with secondary infections, affecting individuals unaware of their prior asymptomatic infections [4].

Antibody-dependent enhancement (ADE) is the proposed mechanism behind this increased severity. In ADE, sub-neutralizing antibodies from the primary infection can provide better entry of virions through Fc receptors on monocytes, leading to higher viral load, excess inflammatory cytokine secretion, and severe disease manifestations [5]. The issue became more concerning with the use of the live-attenuated Dengvaxia vaccine, which yielded suboptimal outcomes in naïve individuals. For those without prior exposure, vaccination was associated with an increased risk of severe dengue fever, potentially due to ADE [6].

The urgent need for effective preventive measures against dengue highlights the importance of developing an animal model capable of recapitulating severe dengue fever for preclinical vaccine testing. Growing evidence supports the protective role of CD8+ T cells in dengue infection [7], and a CD8+ T cell targeting mRNA vaccine has already been patented, showing promising results in human HLA transgenic mice [8, 9]. A comprehensive animal study focusing on controlling severe dengue manifestations through ADE will be a critical step toward translating these findings into clinical applications.

Objective

Our overall objective is to study the manifestations of severe dengue disease, including the immune response to infection, in a murine model to facilitate preclinical vaccine testing.

Research Hypothesis

Type-I interferon receptor knockout would render IFNAR1-/- mice susceptible to dengue infection while C57BL/6 wild-type controls would remain resistant. In addition, by administering anti-flavivirus antibodies prior to infection, IFNAR1-/- mice would demonstrate a more severe disease phenotype compared to a non-ADE condition. Additionally, we propose that type-I interferon receptor knockout mice possess immunological activities of DENV-targeting CD8+ T lymphocytes post infection.

Research Aims

1. Establish a model of severe dengue disease using IFNAR1 -/- C57BL/6 mice under antibody-dependent enhancement.
2. Characterize disease phenotypes including survival, morbidity rate, viral load, vascular leakage, and inflammatory cytokines.
3. Evaluate the immune response post infection and focus on CD8+ T lymphocytes in severe dengue disease model.

Comprehensive Literature Review

Transmission of Dengue Virus Based on differences in their surface structures, dengue virus (DENV) is classified into four serotypes (DENV-1 to DENV-4), which interact differently with antibodies present in the host sera and share approximately 65% of their genome [10]. DENV-1-4 are hypothesized to have originated from a common sylvatic DENV ancestor strain,

transmitted by canopy-dwelling *Aedes* genus mosquitos in individual events, and evolved in nonhuman primates in West Africa and Malaysia [11]. The geographical prevalence of each DENV serotype varies slightly, but collectively, these strains are predominantly found in tropical regions [12]. A dengue burden prediction made in 2010 highlighted South Asia, Southeast Asia, and Latin America as the three regions around the world with the highest disease occurrence [2]. Recent trends, however, suggest that DENV is expanding beyond tropical areas [13, 14]. Increasing vector densities, population growth, international travel, and virus evolution all contribute to the rising burden of dengue infection globally [15]. In addition, mosquito-borne diseases are now reaching higher altitudes and temperate regions, potentially due to climate change extending the length of the transmission season and increasing the number of people at risk of DENV [16, 17].

DENV is primarily transmitted between humans by *Aedes aegypti* and *Aedes albopictus* mosquitos that have adapted well to urban environments and feed on human blood [10, 18]. The DENV transmission cycle starts when a female mosquito bites an infectious host, allowing the virus to spread and multiply in the mosquito's midgut before migrating to various tissues, including the salivary gland [19]. This extrinsic incubation period, which takes around 8-12 days, ends when the mosquito becomes infectious [20]. It remains infectious for the rest of its life, which typically lasts less than two weeks [19, 20].

Therefore, an important factor influencing mosquito transmission is the length of the extrinsic incubation period, which is tightly linked to temperature [21]. Higher ambient temperatures have been shown to accelerate the virus's extrinsic incubation time, reducing the period required for a mosquito to become infectious [22]. For example, while the incubation period for *Aedes aegypti* was 12 days at 30 ^{o}C, it was shortened to 7 days at 32-35 ^{o}C [22]. Notably, DENV transmission to monkeys by mosquitos only occurred at temperatures above 30^{o}C [22], further emphasizing the role of climate change in transmission dynamics.

In 2023, the Americas recorded over 4.6 million cases of dengue fever, with nearly 45% confirmed through laboratory testing [23]. Although Canada does not have endemic dengue, diagnosed cases among the 8 million travelers returning from endemic countries, such as Caribbean, Cuba, and Mexico are on the rise [24-27]. In addition, since 2018, the establishment of *Aedes* mosquitos in southwestern Onterio indicates that local transmission is now a possibility [28]. Thus, despite Canada's relatively low incidence, it is not immune to the global threat posed by DENV, necessitating increased vigilance and preventive measures.

Virology Dengue virus (DENV) is a member of the Flaviviridae family, which includes yellow fever virus (YFV), West Nile virus (WNV), Zika virus, and Japanese encephalitis viruses (JEV) [29]. The DENV genome consists an 11 kb positive-sense, single-stranded RNA molecule which encodes one polyprotein that is processed into three structural proteins (the capsid (C), envelope (E), and pre-membrane/membrane (prM/M) proteins) and seven non-structural proteins (NS1, NS2A, NS2B, NS3, NS4A, NS4B, and NS5) [30, 31]. The structural proteins form the virion particles, while the non-structural proteins are essentials for viral RNA replication, polyprotein processing, and immune evasion within an infected cell [31].

Several ubiquitous cell-surface protein candidates - such as heat-shock protein 70 in mosquito cells and C-type lectin receptors (e.g., DC-SIGN) in human myeloid cells - have been identified to interact with DENV envelope protein and allow receptor-mediated endocytosis; however, a *bona fide* flavivirus receptor has not been identified [32, 33]. On the other hand, when DENV viruses are opsonized by antibodies that do not neutralize their infectivity, they can enter mononuclear lineage cells, including monocytes, macrophages, skin-resident Langerhans cells, and dendritic cells [34], which contain Fc receptors, via FcR-mediated uptake. Therefore, heterotypic DENV antibodies with less optimally to DENV strains or DENV antibodies at sub-neutralizing concentrations could enhance the entry of viruses.

The intracellular replication cycle of dengue virus begins when virions are internalized

into acidic endosomes [35]. The low pH induces conformational changes in the viral envelope protein, promoting fusion between the viral and vesicular membranes, which releases the nucleocapsid into the cytoplasm [36]. The viral RNA is then translocated to the endoplasmic reticulum, where it undergoes translation with the help of host protein complexes [35]. Each of the structural and non-structural dengue proteins has been implicated in multiple functions [37]. Specifically for viral genome replication, the NS2B-NS3 protease complex processes the polyprotein at several cleavage sites, primarily at the junctions of the nonstructural proteins [38]. Similarly, NS5 serves as a RNA-dependent RNA polymerase, synthesizing the negative mRNA strand using the positive sense mRNA as a template during genome replication [39]. After rounds of RNA synthesis, viral structural proteins encapsulate the viral genome, assembling it into virions that are then transported through the Golgi apparatus [37]. The acidic environment of the Golgi exposes the furin cleavage site in prM to ensure proper virion maturation and infectivity [40].

A DENV protein that has been linked with disease pathology is the secreted form of non-structural protein 1 (NS1) hexamer, which is also a diagnostic biomarker for early acute infection as its levels correlate with viremia and disease severity in secondary dengue infection [41]. In addition, NS1 acts as a pathogen-associated molecular pattern (PAMP) and directly activates mouse macrophages and human peripheral blood mononuclear cells (PBMCs) via Toll-like receptor 4 (TLR4) [42]. This activation leads to the release of proinflammatory molecules such as tumor necrosis factor alpha (TNFα) and monocyte chemoattractant protein 1 (MCP-1) that have been implicated in inducing the loss of vascular endothelial cadherin and leads to increased endothelial layer permeability when supplementing them to human vein endothelial cells [42-45]. However, the exact mechanism by which NS1 induces endothelial barrier dysfunction needs to be further studied.

Clinical Manifestation In the majority of the patients with primary DENV infection, the

infection remains asymptomatic, while the rest suffer from mild fever and flu-like symptoms such as fatigue, headache, and myalgia [46]. Primary infection with one strain of DENV elicits a homotypic immune response that generates neutralizing antibodies specific to that strain. However, these antibodies do not confer long term cross-protection against subsequent infections caused by the other three DENV strains [46, 47]. Thus, an individual with a secondary heterotypic dengue infection has a higher chance of getting severe forms of dengue, dengue hemorrhagic fever (DHF) and dengue shock syndrome (DSS), which can lead to thrombocytopenia, internal bleeding, organ failure, and death [46].

According to the World Health Organization 1997 guidelines for dengue, DHF is characterized by vascular permeability defects, multifactorial hemostatic abnormalities, and bleeding diathesis, with severe cases classified as DSS [48]. The decline in platelet count usually precedes vascular leakage and can be used as an indicator for determining whether to hospitalize suspected DHF patients [49]. As it was difficult to apply the original classification clinically, in 2009, a new classification system defined patients as having probable dengue, dengue with warning signs, or severe dengue [50]. This classification allows clinicians to assess the likelihood of a febrile person visiting or living in dengue-endemic region being diagnosed as a new dengue case based on the severity of the symptoms, which range from nausea and vomiting, to mucosal bleeding and liver enlargement, to fluid accumulation with severe haemorrhage [50].

It has been repeatedly reported that subsequent heterologous dengue infections result in a higher rate of DHF in populations with non-neutralizing, heterotypic DENV antibodies, a phenomenon known as antibody-dependent enhancement (ADE) [47]. Studies have been conducted to characterize these antibodies by comparing their quantity, immunoglobulin isoforms, and neutralizing abilities in patients with inapparent dengue fever versus DHF. When simply comparing anti-DENV Immunoglobulin G (IgG) titer and neutralizing antibody titer in

hospitalized and inapparent dengue patients, one might conclude that higher titers are found in hospitalized dengue patients for both measurements [51]. However, a closer look at patients with primary or secondary dengue infections reveals that high levels of anti-DENV IgG and neutralizing antibody titers correlate with secondary dengue infection in both hospitalized and inapparent dengue patients [51]. Additionally, it was discovered that DHF patients had IgGs with enhanced affinity for FcγRIIIA expressed on monocytes, macrophages, and natural killer cells [52]. This enhanced affinity is due to the removal of fucosylation on the Fc domain of these antibodies and is positively correlated with disease severity [52].

Severe dengue during a primary infection has been observed in infants born to mothers with pre-existing dengue immunity [53]. These infants are at high risk for severe dengue due the decay of maternal derived antibodies 6-9 months after birth, which leads to sub-neutralizing levels of DENV-targeting antibodies [54]. This epidemiological discovery was validated in an animal model of severe dengue disease, where DENV 2 infections were modeled in mice born to DENV 1 immune mothers [55]. Higher viremia and increased vascular leakage were found compared to those born to dengue naïve mothers [55]. Furthermore, the severe disease manifestation was age dependent, with 2-week-old mice being significantly more protected against heterotypic DENV infection than 8-week-old mice [55]. To summarize, these findings support the hypothesis that preexisting, heterotypic DENV antibodies at sub-neutralizing level contribute to severe dengue disease pathogenesis.

Immune Response Dengue infection in humans begins when a mosquito takes a blood meal and inoculates the virus subcutaneously. The infection of skin-resident immune cells triggers an innate immune response via pathogen-recognizing receptors (PRRs) such as retinoic acid-inducible gene I (RIG-I), melanoma differentiation-associated protein 5 (MDA5), and Toll-like receptor 3 (TLR3) [56]. For instance, when dengue virus infects myeloid dendritic cells, PRRs recognize the double-stranded RNA produced during viral replication as PAMPs

[56]. This recognition initiates a signaling cascade that drives these cells to differentiate into activated-mature myeloid DCs expressing markers such as CD80, CD86, and CD83 and stimulates the production of TNFα and IFNα [57]. TNFα increases the expression of E-selectin on blood vessels, which recruits circulating monocytes to the site of infection [58]. IFNα binds to IFNAR1 and activates the Janus kinase/signal transducer and activator of transcription (JAK-STAT) pathway and leads to the expression of interferon-stimulated genes (ISG) [59].

Activated DCs also act as antigen presenting cells (APCs) and migrate from peripheral tissues to regional lymph nodes where they activate T lymphocytes in T cell zones to initiate the adaptive immune response [60]. In humans, CD4+ T cells are polarized to a T helper 1 (Th1) phenotype, secreting Th1-associated cytokines such as IFNγ, TNFα, and IL-2 after exposing to dengue virus [61]. This promotes the expansion and activation of cytotoxic CD8+ T cells that involve in direct killing of DENV-infected cells [62]. A clinical study enrolling Thai children with acute febrile illnesses confirmed the expansion of DENV-specific CD8+ T cells during acute dengue infection [63]. In a mouse model study, dengue infection results in cytotoxic CD8+ T cells that produce IFNγ and TNFα and are capable of killing DENV peptide-pulsed cells *in vivo* [64]. Activation of humoral immunity leads to the production of neutralizing antibodies that block DENV infectivity and mediate dengue clearance by antibody dependent cellular cytotoxicity (ADCC) [60].

At the same time, the activation of cellular and humoral immune responses has also been linked to the development of severe dengue disease manifestations. In ADE, the presence of heterotypic antibodies at sub-neutralizing concentrations has been associated with exacerbated disease in secondary dengue patients [47]. Another perspective on this phenomenon is the theory of “original antigenic sin,” which proposes that when the immune system is re-exposed to a similar epitope, it mounts a response that depends on the memory of the earlier infection rather than a new primary response, resulting in a faster response [65]. This leads to the

expansion of low avidity B and T cells, which can hinder the efficient clearance of dengue-infected cells [65]. Given the complexity and limited understanding of the immune response to dengue infection, vaccine design has faced difficulties, further emphasizing the importance of an enhanced disease animal model.

Dengue Vaccine Overview Currently, there are no specific antiviral drugs for dengue infection. During the febrile phase of dengue fever, the WHO guidelines on clinical management of dengue advice patients to maintain adequate fluid intake, especially for those experiencing plasma leakage [50]. In an effort to prevent dengue infection, a tetravalent live-attenuated vaccine, CYD-TDV (Dengvaxia), incorporates the pre-membrane (prM) and envelope (E) protein-coding homologous sequences from all four dengue strains into a yellow fever vaccine virus genome [66]. Although the vaccine is approved by Centers for Disease Control and Prevention (CDC) in endemic countries, a case-cohort study that retrospectively analyzed the data from clinical trials of CYD-TDV showed a higher risk of hospitalization among seronegative vaccine recipients compared to seropositive vaccine recipients [6]. Since CYD-TDV is thought to increase the risk of severe dengue disease through the production of dengue neutralizing antibodies eliciting ADE mechanisms in DENV naïve individuals, it is only recommended for individuals with a prior DENV infection [66, 67].

Other vaccine candidates are in various stages of clinical trials. The TAK-003 vaccine (Qdenga) was approved in the European Union in December 2022 and was prequalified by the WHO on May 10, 2024. Similar to CYD-TDV, it is a tetravalent live-attenuated vaccine consisting of virus chimeras. However, it uses the DENV 2 virus as its genetic backbone and replaces the prM and E genes of DENV 2 with those from DENV 1, 3, and 4 strains [68]. In a phase 2 trial, 2-17 year-old participants received either TAK-003 or placebo and showed that TAK-003 elicited tetravalent antibody response against all four dengue serotypes 48 months after vaccination [69]. In addition, no vaccine-related DHF was reported during the 48-month

follow-up period for children living in dengue-endemic countries. In a phase 3 trial, TAK-003 has high vaccine efficacy (diagnosed dengue cases in placebo recipients compared to TAK-003 recipients in the 17-month observation period) for DENV 2 (95.1%), but less protection for DENV 3 (48.9%) [70]. Even though CYD-TDV and TAK-003 both demonstrated a certain level of vaccine efficacy, these vaccines are composed of attenuated viruses and are not recommended for immunocompromised population.

To circumvent priming seronegative individuals with DENV surface proteins, a mRNA DENV-NS poly-epitope vaccine consisting of conserved peptides from the non-structural proteins, NS3-NS4B-NS5, has been produced [8]. These non-structural DENV proteins are not exposed on the surface of DENV virions, which should preclude the production of neutralizing DENV-specific antibodies following vaccination with DENV-NS poly-epitope vaccine [8]. Preliminary study in immunocompetent HLA transgenic mice has shown promising results in eliciting a strong DENV-specific CD8+ T cell response without inducing virus-neutralizing antibodies [8]. Furthermore, immunized mice have reduced titer when challenged with DENV compared to those receiving control mRNA peptides [8]. Therefore, assessing the vaccine's ability to modulate severe dengue pathogenesis is a crucial step towards clinical trials and the development of a safer dengue vaccine.

Dengue Infection Mouse Models Modeling dengue disease in laboratory animals has been challenging as DENV naturally infects only primates [71]. Infecting non-human primates (NHPs) with clinical DENV strains can result in viremia [71]. Species such as chimpanzees and marmosets, which possess humoral immunity similar to that of humans, are thus valuable for assessing the neutralizing antibody response in vaccines efficacy studies [72, 73]. However, the use of NHPs presents several drawbacks, including ethical constraints, inconsistencies in disease manifestations among individuals, and the limited availability of these animals [71]. These challenges have driven the development of rodent models for studying dengue infection.

However, most immunocompetent adult mice do not exhibit significant disease symptoms when inoculated with clinical DENV isolates via peripheral routes [74]. This limitation has driven the need for murine models with altered immune systems, particularly focusing on the type I interferon signaling pathway. DENV has evolved mechanisms to suppress this pathway, which is key to antiviral defense. For example, the DENV nonstructural protein 5 (NS5) degrades STAT2 protein, a critical component of the type-I interferon pathway, in human cells but not in murine cells [75]. Another study reported that the DENV NS2B-NS3 protease complex can cleave the human stimulator of the interferon gene protein (STING), which contributes to detecting viral DNA and cyclic di-nucleotide PAMPs, but not mouse STING [76].

Therefore, researchers developed the AG129 mouse model, which lacks both type I interferon alpha/beta (IFNα/β) and type II interferon gamma (IFNγ) receptors [77]. This model is susceptible to DENV infection and has been widely used to assess the effects of antiviral treatments in lethal dengue challenge studies [78, 79]. Moreover, an enhanced dengue disease is seen after passive transfer of heterologous DENV serum prior to infection, which suggest the AG129 model can achieve antibody-dependent enhancement that leads to severe dengue disease in human [80]. Despite these advantages, the absence of IFNγ signaling, which is critical for the activity of anti-DENV CD8+ T cells, limits the utility of this model for studying the full spectrum of immune responses against DENV [81].

To explore the dengue disease phenotype in a less immunocompromised model, researchers utilized mice lacking only the type-I interferon alpha/beta receptor (IFNAR1-/-) [82]. This model retains more immune functionality while maintaining susceptibility to DENV infection. Studies using this strain of mice have demonstrated that these mice succumb to mouse-adapted DENV infection, exhibiting morbidity, high viral loads in serum, and excretion of inflammatory cytokines [83-85]. Nevertheless, some researchers remain skeptical about this

model due to concerns about its incomplete immune response. Consequently, alternative approaches have been explored to address these limitations.

One alternative involves transiently inhibiting IFNAR1 in C57BL/6 mice with antibodies one day prior to infection, allowing DENV to enter and replicate while retaining a functional immune system [8]. This model enables monitoring of viral titer and correlating vaccination with a reduction in viral load and disease prognosis. However, this model does not replicate human dengue symptoms, and viral titers do not directly reflect disease severity, limiting its utility for clinical translation.

Another approach involves cell-specific IFNAR1 knockout using the Cre-lox system. For instance, conditional deletion of IFNAR1 expression in $CD11b^{hi}CD11c^{lo}$ macrophages in LysM Cre^{+}*Ifnar*$^{f/f}$ mice allows dengue infection to be established and results in detectable viral titers, though at lower levels than in IFNAR1-/- mice [86]. However, there are caveats to the cell-specific IFNAR1 knockout, as macrophages play a crucial role as antigen presenting cells in the adaptive immune system, leading to potential immune deficiencies and unknown effects. To address these concerns, an inducible Cre-lox system, where the knockout only takes place when administering tamoxifen, has been proposed. This approach may provide a severe dengue model allowing for direct vaccination of the mice. While promising, the development and validation of such a model in dengue vaccine trials would require additional time.

Ultimately, IFNAR1-/- mice offer the most practical balance between immune functionality and susceptibility to DENV infection. Further investigation is needed to better understand the antiviral immune response, particularly the role of cytotoxic T cells, which contribute to the clearance of DENV-infected cells through both direct killing and the release of cytokines such as IFNγ and TNFα [87]. This makes IFNAR1-/- mice an ideal platform for advancing our understanding of severe dengue pathogenesis while maintaining a relevant immune profile.

Chapter II: materials and methods

Virus Stock Production

Sujan Shresta from the La Jolla Institute for Immunology, CA, USA, kindly provided the D220 mouse-adapted DENV-2 strain [83]. Briefly, the PL046 strain, a clinical DENV2 isolate, was originally obtained from Dr. H.-Y. Lei at National Cheng Kung University, Taiwan [88]. This strain was alternatively passed between AG129 mice and C6/36 cells 20 times, resulting in the novel DENV2 strain, D220. The D220 strain was propagated at McGill University at a multiplicity of infection (MOI) of 0.01 using C6/36 cells, isolated from larva of an Asian tiger mosquito, cultured at 28ºC without carbon dioxide in L-15 medium supplemented with 10% fetal bovine serum (FBS), 1% penicillin/streptomycin, 1% non-essential animal acids, and 1% tryptose phosphate broth (TPB). Viral absorption was allowed for 2 hours at 28ºC. Afterward, 10 mL of L-15 medium containing 2% FBS, 1% penicillin/streptomycin, 1% non-essential animal acids, and 1% TPB was added to each T150 flask. Two days post infection, the medium was replaced with fresh L-15 medium with the same composition. The viral supernatant was harvested from flasks where over 90% of cells showed lysis. The supernatant was then centrifuged at 4,000 g for 15 minutes using Amicon Ultra-15 Centrifugal Filters and aliquoted for future use.

Infectious Virus Titrations

Plaque assay and focus forming assay were done in parallel to validate the viral titer.

Plaque assay

One day prior to infection, $6x10^5$ Vero cells per well were seeded in 6-well plates. On the day of infection, the cells were washed with plain Dulbecco's Modified Eagle Medium (DMEM). The viral stock was then serially diluted 10-fold in plain DMEM, ranging from 10^{-1} to 10^{-8}. A volume of 400 µL from each viral dilution was added per well. Viral absorption was allowed for 2 hours. After absorption, the virus was removed and replaced with carboxymethylcellulose

(CMC) mix consisted of a 1:1 ratio of CMC solution (prepared by dissolving 32 grams of CMC and 8.5 grams of sodium chloride in 1 liter of distilled water) and DMEM supplemented with 2% FBS and 1% penicillin/streptomycin at 37 °C. Ten days post infection, the CMC mix was removed, and the cells were fixed with 10% formalin for 20 minutes. The wells were then stained with crystal violet for 20 minutes, washed with distilled water, and the plaque forming units (PFU) per milliliter of virus were calculated based on the number of plaques observed.

Focus forming assay

$3x10^4$ Vero cells per well were seeded in 96-well plates. The infection procedure followed the same steps as the plaque assay, except that 40 µL of each viral dilution was added per well. After 2 hours of viral absorption, the virus was removed and replaced with CMC solution, and the plates were incubated at 37 °C. Three days post infection, the cells were fixed with 4% formaldehyde for 20 minutes. Each well was permeabilized with 50 µL of 0.3% Triton X-100 and 5% FBS in phosphate buffered saline (PBS) for 20 minutes. Subsequently, 40 µL of a 1:500 dilution of the Flavivirus group antigen Antibody (D1-4G2-4-15 (4G2)) was added to each well and incubated for 1 hour at 37°C. The cells were washed three times with PBS, followed by the addition of 1:500 Goat anti-mouse IgG (H+L) Alexa Fluor 488 secondary antibody, and incubated for 45 minutes at 37°C. After three washes with PBS, the fluorescent foci were counted using a Zeiss Axiocam 305 mono fluorescent microscope. Focus forming units (FFU) per mililiter of virus were calculated based on the number of foci observed.

Mouse Breeding & Genotyping

B6.129S2-Ifnar1^{tm1Agt}/Mmjax (strain number 032045), which lack type-I interferon receptor function, were purchased from Jackson Laboratories (Bar Harbor, ME, USA).

These IFNAR1 knockout mice were bred with CD8-/-: B6.129S2-*Cd8a*^{tm1Mak}/J (strain number 002665), a CD8+ T cell knockout strain also obtained from the Jackson Library [89], to generate a double knockout strain. Genotyping was performed following the protocols

provided by Jackson Laboratories. All animal procedures were conducted under the approved animal use protocol 4792 from the McGill University Animal Care Committee.

In Vivo Infections

Mice were intravenously injected with 200 µL of D220 virus, diluted in sterile PBS, per mouse. To model antibody-dependent enhancement (ADE), mice were administered 10 µg of anti-flavivirus envelope protein antibodies (Flavivirus group antigen Antibody D1-4G2-4-15 [4G2]) intraperitoneally, in a 200 µL inoculum per mouse, one day prior to DENV infection. The mice were monitored daily for clinical signs and body weight changes. Animals were humanely sacrificed if their body weight decreased by over 20%, in accordance with animal use protocol 4792, approved by the McGill University Animal Care Committee.

Evans Blue

Mice were injected intraperitoneally with 200 µL of 1% Evans blue dye (E2129, Sigma-Aldrich) prepared in PBS. One day later, the mice were perfused with 12 mL of PBS through the left ventricle. Tissues were then collected in pre-weighted 1.5 mL Eppendorf tubes containing 500 µL of 99.5% formamide and incubated at 55^{o}C for 24 hours. The Evans blue concentrations in the formamide extracts were quantitated by measuring absorbance at 610 nm, using formamide alone as the blank.

RNA Extraction & qRT-PCR

Sera and tissue samples were processed using the QIAamp Viral RNA Mini Kit (52906, Qiagen), following the manufacturer's protocols. Cycle threshold (Ct) values were converted to RNA concentrations (ng/ µL) by a DENV-specific RNA standard built in house. Results were normalized to viral genome equivalents per milliliter of serum. The limit of detection value (45 cycles) was extrapolated based on viral RNA copies per mL, as determined by the DENV-specific RNA standard established for each reaction plate.

$$\frac{\text{concentration of RNA } (\frac{\text{ng}}{\mu\text{L}}) \times \text{Avogadro's number}}{\text{molecular weight of transcript } (\frac{\text{g}}{\text{mol}}) \times 1{,}000{,}000{,}000} = RNA\ copies/\mu L$$

Equation for converting concentration of RNA-to-RNA copies per microlitre is adapted from Case, J.B., et al. [90]. Concentration of RNA is quantified by NanoDrop spectrophotometer. Since we know the exact length of the RNA sample, the molecular weight can be calculated by multiplying the total number of base pairs by 660 g/mole (average weight of dsDNA).

Plasma Cytokine Analysis

Plasma was obtained by adding whole blood to tubes containing 1.6 mg/ml ethylenediaminetetraacetic acid (EDTA) and centrifuging at 3,000 g for 10 minutes at room temperature. Serum samples were virus-inactivated by adding 1% Triton X-100 and incubating for 1 hour at room temperature. Samples were evaluated in Eve Technologies (Calgary, AB, CA) for the Mouse Cytokine Proinflammatory Focused 10-Plex Discovery Assay® Array (MDF10).

Flow Cytometry

Lymphocytes were isolated from spleens by manually dissociating the tissue in Roswell Park Memorial Institute (RPMI) medium with 10% FBS, followed by treatment with 1 mL of RBC Lysing Buffer Hybri-Max (no. R7757; Sigma-Aldrich). For *ex vivo* stimulations, 1 x 10^6 splenocytes were incubated for 4 h at 37ºC in RPMI 10% medium, supplemented with either 1) Cell Stimulation Cocktail (1:500 dilution, 00-4975-93, containing PMA/ionomycin and protein transport inhibitors; eBioscience) or 2) purified CD3ε antibody (clone 145-2C11, 1:250 dilution), purified CD28 antibody (clone 36.51, 1:500 dilution), brefeldin A (1:500 dilution, 00-4506-51; eBioscience), and monensin (1:500 dilution, 00-4505-51; eBioscience). For DENV-specific T cells, the exact peptide sequences used are provided in Supplementary Table 4. 1 × 10^6 splenocytes were stimulated with 2 μg/ml H-2b -restricted epitopes in the presence

of brefeldin A for 5 hours at 37ºC in RPMI 10% medium. These stimulated cells were then stained extracellularly, fixed and permeabilized using the Foxp3/Transcription Factor Staining Buffer Set (00-5523-00; eBioscience) according to the manufacturer's instructions, and finally stained intracellularly for IFN-γ expression.

For extracellular and intracellular staining, the following fluorochrome-conjugated antibodies were used: Fixable Viability Dye eFluor506 (65-0866-14; eBioscience) was used to identify dead cells, CD45 FITC (103108; BioLegend), TCRB eFluor 450 (48-5961-80; eBioscience), IFN-γ APC (17-7311-82; eBioscience), CD8a BV785 (417-0081-80; eBioscience), CD4 APC-ef780 (47-0041-82; eBioscience), CD44 PerCP-Cy5.5 (45-0441-80; eBioscience), CD62L PE (12-0621-81; eBioscience), NK1.1 PE-Cy7 (25-5941-82; eBioscience). DENV-specific tetramers were customized from NIH Tetramer Core Facility at Emory University. MHC allele H2-Kb was used for DENV C 51-59, H2-Db for NS4B 66-74 and NS4B 99-107. The above three peptides were labeled with APC. MHC allele H2-Db was used for SARS-CoV-2 N 219-227 and labeled with PE. A total of $1x10^5$ events per sample were acquired on a BD LSRFortessa and gated as described in Supplemenary Figure 3 with FlowJo version 10.10.1 software.

Statistical Methods

All statistics were calculated using GraphPad Prism version 9.0.2 (GraphPad Software, San Diego, California, USA). Significance levels were defined as p*<0.05, p**<0.01, p***<0.001, and p****<0.0001. The nonparametric Mann-Whitney U test was used for comparisons between two groups, while the Kruskal-Wallis H test, followed by Dunn's multiple comparison test was used for multiple groups.

Chapter III: results

Type I interferon-α/β receptor knockout mice (IFNAR1 -/-) is a model of fatal antibody-dependent enhancement (ADE) upon dengue infection To achieve our research aims, we challenged IFNAR1-/- mice with mouse-adapted dengue 2 virus (D220) and monitored their health conditions compared to wild-type C57BL/6 mice. Each mouse received a viral dose of $1x10^6$ plaque forming unit (PFU) of the D220 strain via intravenous injection. To induce antibody-dependent enhancement (ADE), 10 μg, which is at a sub-neutralizing amount, of anti-flavivirus envelope protein antibody (D1-4G2-4-15, clone 4G2) was administered intraperitoneally one day prior to infection. As demonstrated in Figure 1A and B, IFNAR1-/- mice were susceptible to D220 infection, with several succumbing to the virus and all experiencing transient weight loss, peaking around day 3-5 post infection. In contrast, C57BL/6 wild-type control mice maintained stable body weight with or without ADE. On the other hand, ADE had render IFNAR1-/- mice more susceptible to D220 infection, raising mortality from 20.0% to 71.4%. Convalescent IFNAR1-/- returned to their baseline weight by day 6 post infection.

To attribute the severe dengue symptoms observed to the sub-neutralizing levels of anti-flavivirus antibodies administered to IFNAR1-/- mice, we set up groups of IFNAR1-/- mice that were given 10 μg 4G2 antibodies, 10 μg isotype antibodies (IgG2 isotype control), or 200 μL of PBS. Each mouse received $7x10^6$ PFU, with results shown in Figure 1C and D. Infected IFNAR1-/- mice that were not under ADE (isotype controls: 14.3% mortality; PBS controls: 0% mortality) were much less susceptible to D220 infection compared to ADE mice (4G2 antibodies given: 100% mortality). All infected IFNAR1-/- mice experienced transient weight loss, but ADE mice exhibited much higher morbidity, as shown in Figure 1E. The clinical symptoms demonstrated by infected IFNAR1-/- mice exclusively were inactivity, hunched posture, and ruffled coat, as detailed in Supplementary Table 1 for morbidity scoring standards.

Both male and female mice were included in all infection experiments, with no significant differences observed in any of the measured parameters.

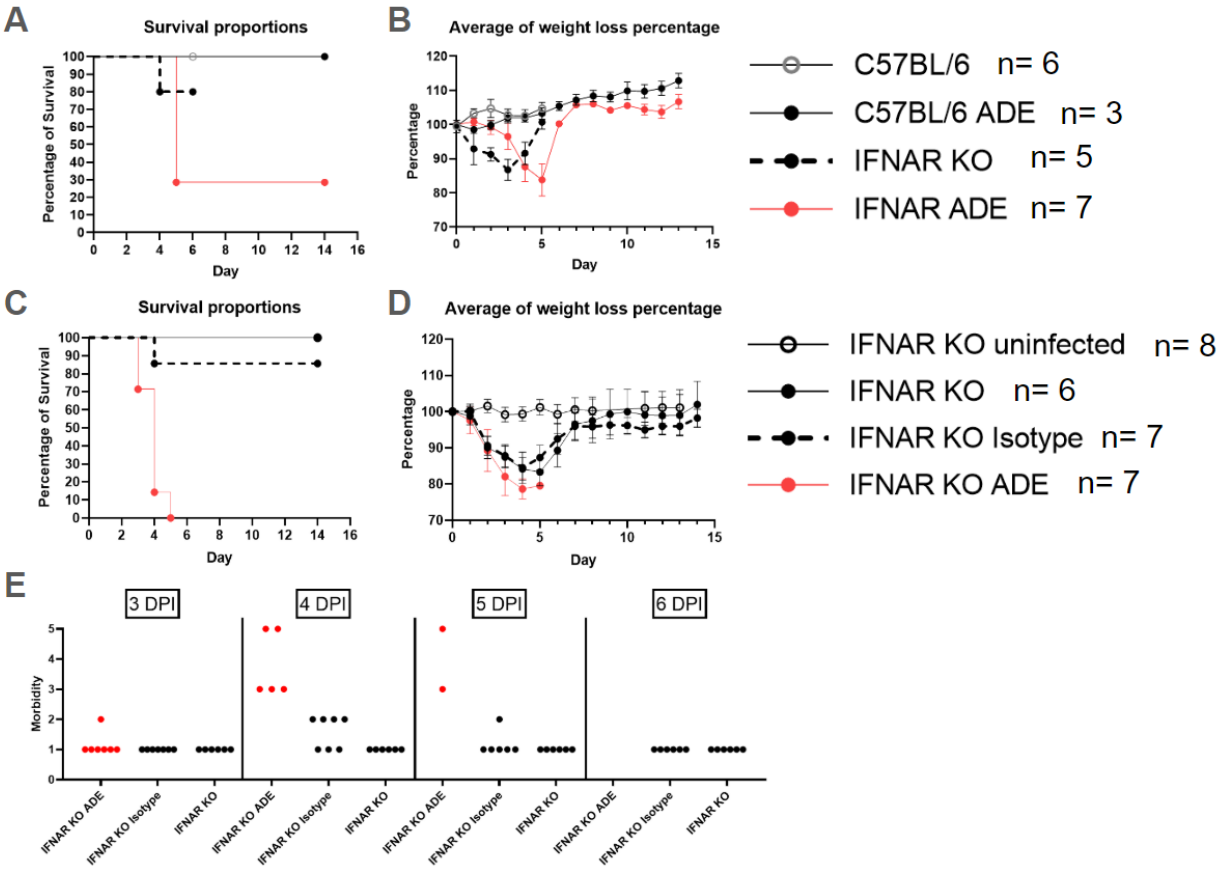

Figure 1. Type I interferon-α/β receptor knockout mice (IFNAR1 -/-) is a model of fatal antibody-dependent enhancement (ADE) upon dengue infection. 20% weight loss was the pre-determined clinical endpoint. **(A)** Percentage of survival showed no wild-type control mouse (n=6) succumbed to D220 mouse-adapted dengue infection, while 1 out of 5 IFNAR1-/- mice succumbed to D220 infection at $7x10^5$ PFU/mouse. At $1x10^6$ PFU/mouse no wild-type control under ADE succumbed (n=3) during the 14-day monitoring period, while 5 out of 7 IFNAR1-/- succumbed to D220 infection. **(B)** Only IFNAR1-/- mice experienced transient weight loss. (**C)** 7 out of 7 4G2 antibodies given IFNAR1-/- mice succumbed, 1 out of 7 isotype antibodies given IFNAR1-/- mice succumbed, and 0 out of 6 PBS given IFNAR1-/- mice succumbed. **(D)** All IFNAR1-/- mice experienced transient weight loss. **(E)** Morbidity of IFNAR1-/- ranged from 1 (healthy) to 5 (death/no mobility). Mice that were humanely sacrificed were removed from the dataset for subsequent days. As all ADE mice reached clinical endpoint, no dots are shown on day 6 post infection.

Vascular leakage in tissues of IFNAR1-/- mice experiencing severe dengue infection.

Next, since vascular leakage is a symptom of severe dengue disease in humans, we aimed to

determine if IFNAR1-/- mice under ADE could recapitulate this clinical feature. Vascular leakage occurs during the acute phase of infection, so we examined the mice at their peak morbidity. On day 3 post infection, we administered 1% Evans blue dye made in PBS intraperitoneally to IFNAR1-/- mice infected with $7x10^6$ PFU under ADE. On day 4 post infection, coinciding with the greatest weight loss and highest morbidity rate, the paws, facial skin, and ears of all mice given Evans blue dye turned prominently blue. Additionally, the peritoneum, small intestine, and large intestine of infected mice (right mouse on Figure 2A and B) was more prominently blue compared to uninfected mice (left mouse on Figure 2A and B), suggesting a more permeable vascular system. This leakage allowed the dye to diffuse into the tissues, which were then incubated in formamide to quantify the dye in the formamide extracts for downstream comparison of dye amounts in these organs. The color difference in the formamide extracts of spleen and liver tissues between infected and uninfected can be visually distinguished (Figure 2C). There was a significant difference in 610 nm optical density (OD) readings of spleen and liver tissues between infected and uninfected IFNAR1-/- mice (Figure 2D and E).

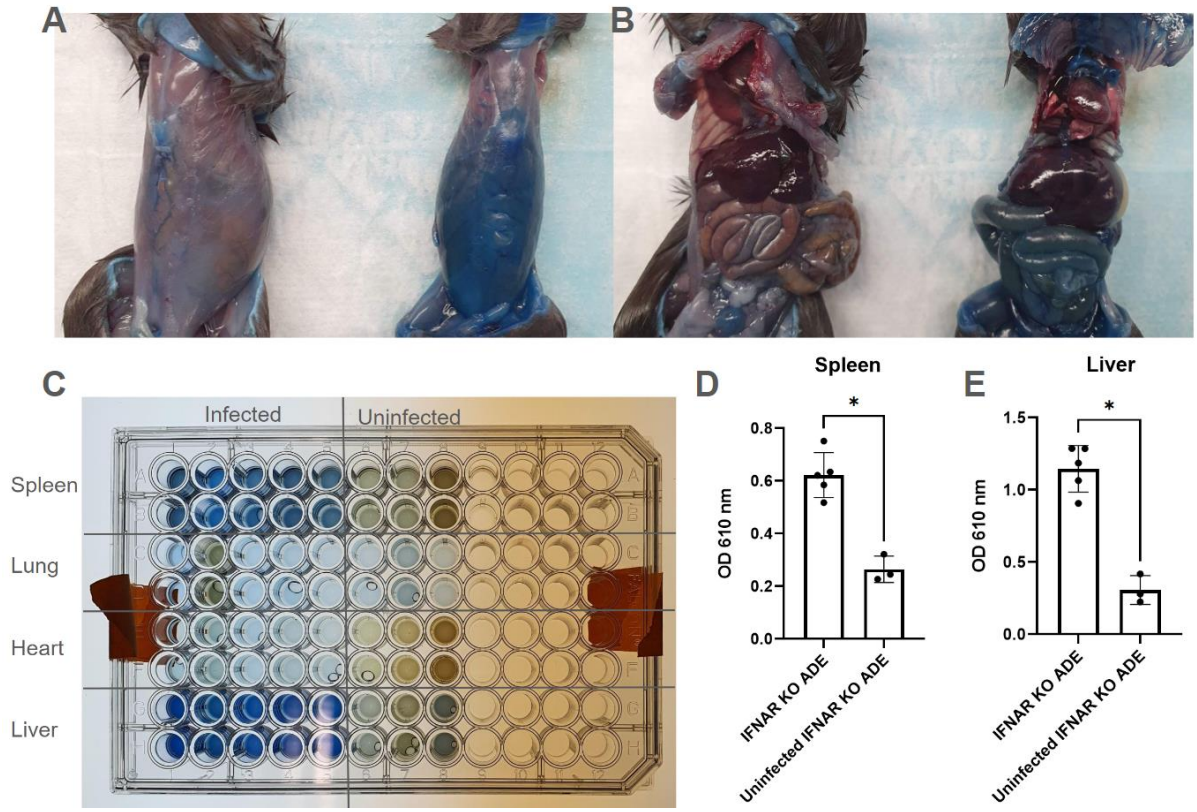

Figure 2. Vascular leakage in tissues of IFNAR1-/- mice experiencing severe dengue infection. (A and B) All mice were perfused with 12 mL PBS through the left ventricle. **(C)** Spleen, liver, lung, and heart tissues were collected and incubated in formamide at 55ºC for 24 hours for the dye to diffuse out from the tissue to formamide. **(D and E)** Evans blue concentrations in formamide extracts were quantitated by measuring absorbances at 610 nm. Formamide alone was blank reading. p*<0.05 using the Mann-Whitney test.

The temporal profile of viral load in serum and spread of virus in organs. In Figure 3A, IFNAR1-/- mice were challenged with $7x10^6$ PFU under ADE. The dynamics of viral titer correlated with the dynamics of weight loss and morbidity, as shown in Figure 1D and E. As the viral titer remained high from day 1-5 post infection, the mice also experienced transient weight loss and clinical symptoms during this period. Next, we compared the viral load in mice given 4G2 antibodies, isotype antibodies, and PBS as a control, all challenged with $7x10^6$ PFU. Despite the higher mortality in IFNAR1-/- mice under ADE, their viral load was comparable to that in IFNAR1-/- mice without ADE (Figure 3B). C57BL/6 mice were not susceptible to D220 infection as they did not experience weight loss (Figure 1B), and their viral load remained undetectable on day 1 and 4 post infection when challenged with $1x10^6$ PFU (Figure 3C).

We then compared the viral load in RNA extracted from different tissues (spleen, lung, liver, and bone marrow) and hypothesized that the virus would disseminate from blood (the virus was administered intravenously) to the rest of the body if IFNAR1-/- mice were permissive to D220 infection. There was detectable viral load in serum, bone marrow, liver, spleen, and lung extracts from IFNAR1-/- mice at $1x10^6$ PFU of D220 (Figure 3D). To summarize, all infected IFNAR1-/- mice are susceptible and permissive to D220 infection as they demonstrated elevated levels of DENV detection during the peak of infection. In contrast, immunocompetent C57BL/6, which do not sustain dengue infection or signs of disease, showed viral loads close to the limit of detection, comparable to those in uninfected mice.

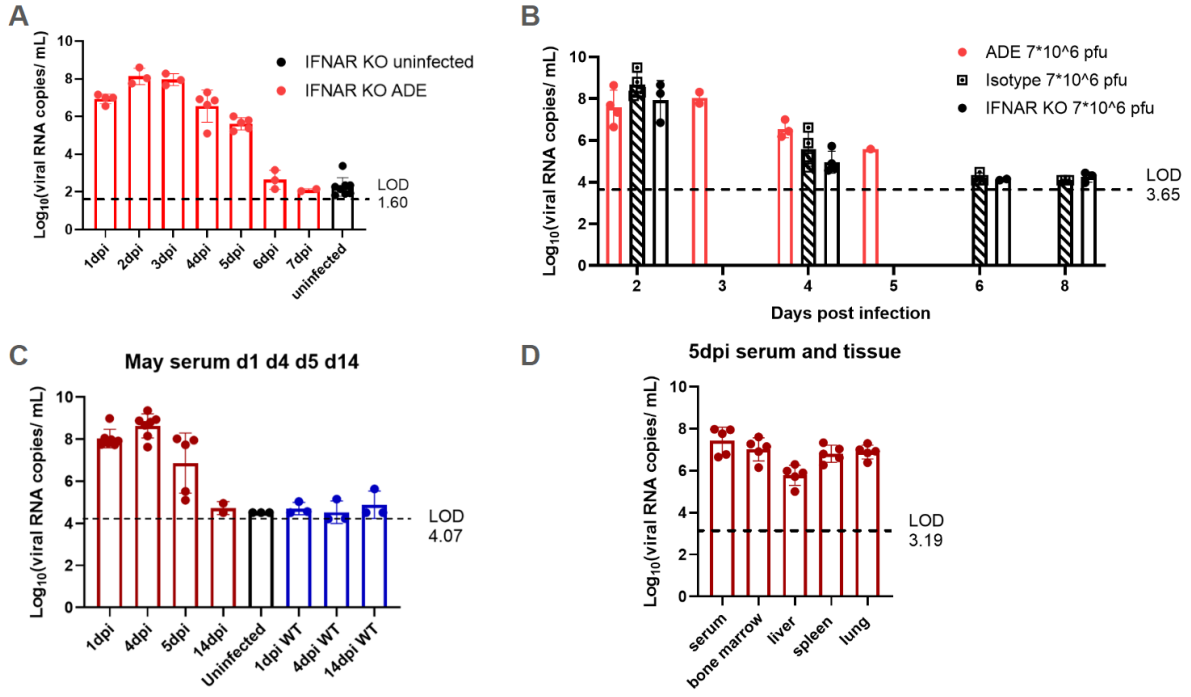

Figure 3. The temporal profile of viral load in serum and spread of virus in organs. (A) In a single experiment, 10 IFNAR1-/- mice were infected and divided into three cohorts. Viral titers were measured at specific time points using submandibular bleeding. On days 1, 4, and 7 post-infection (dpi), blood samples were collected from the same 4 mice. On days 2 and 5 dpi, samples were collected from 3 mice in cohort 2, and on days 3 and 6 dpi, the remaining 3 mice were sampled. **(B)** Even though we would like to track the viral load dynamics on a daily basis, it is not possible to perform submandibular bleeding consecutively to the same mouse due to the need to minimize stress and prevent excessive blood loss. We then decided to examine the viral load on the peak of infection (day 2 and 4 post infection) and on the mice that succumbed from D220 infection. **(C)** Viral RNA copies detected in IFNAR1-/- mice infecting with $1x10^6$ PFU of D220 were 10,000-fold more than B6 wild-type controls and

uninfected IFNAR1-/- controls on 4 dpi. **(D)** The figure shows viral RNA copies per mL of serum or cell supernatant from tissue samples.

Proinflammatory cytokine quantification at the acute phase of D220 infection

Another parameter for evaluating infection and immune response is the level of proinflammatory cytokines/chemokines in the serum of our mouse model. We focused on the acute phase of infection (day 4 post infection) and compared ADE IFNAR1-/- to non-ADE IFNAR1-/- mice, as well as ADE IFNAR1-/- to ADE C57BL/6 wild-type mice. All infected mice were given $7x10^6$ PFU of D220. Notably, levels of interferon gamma (IFN-γ), interleukin-6 (IL-6), monocyte chemoattractant protein (MCP-1), and tumor necrosis factor alpha (TNF-α) were elevated in all infected IFNAR-/- compared to wild-type control and uninfected mice (Figure 4). However, only the increase in TNF-α reached statistical significance, likely due to the limited sample size.

To elaborate on the function of these signaling proteins, the presence of IFN-γ suggests an active antiviral immune response, while elevated of IL-6 and TNF-α indicate an inflammatory response [91]. Detection of MCP-1 may indicate recruitment of monocytes to the site of infection or inflammation [92]. Further investigation is needed to understand the specific mechanisms that stimulate the production of these molecules. For the purposes of building a DENV-susceptible mouse model, we have observed an elevation in cytokine secretion between mice susceptible to D220 infection and wild-type mice post D220 infection, while there was no significant difference between ADE and non-ADE IFNAR1-/- mice.

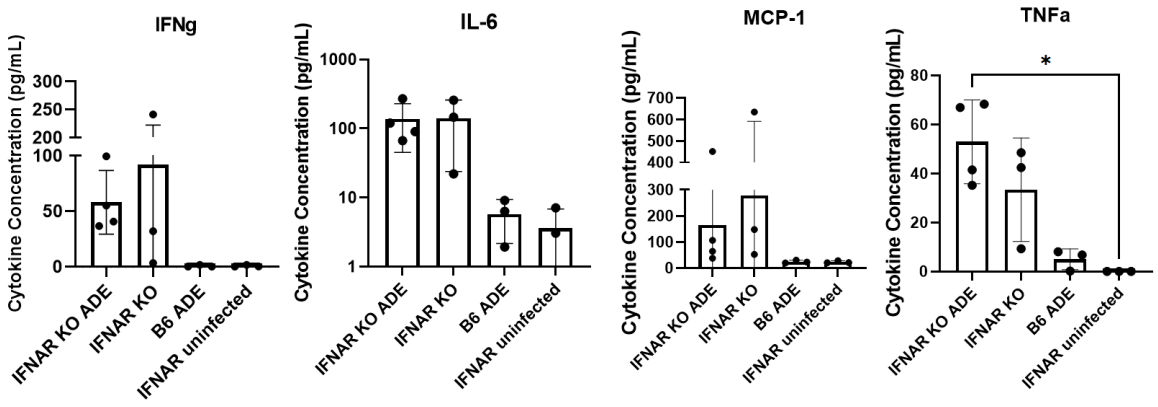

Figure 4. Proinflammatory cytokine quantification at the acute phase of D220 infection. Serum samples from mice infected with $7x10^6$ PFU were collected at 4 dpi and evaluated in Eve Technologies (Calgary, AB, CA) for the Mouse Cytokine Proinflammatory Focused 10-Plex Discovery Assay. p*<0.05, using Kruskal-Wallis test and Dunn's multiple comparison test.

Immune cell dynamics in IFNAR1-/- mice post D220 infection. We detected a trend towards elevated levels of IFNγ, a crucial mediator driving the activation of immune response, in the circulation of infected IFNAR1-/- mice (Figure 4). We next aimed to explore the possible producers of this inflammatory cytokine and focused on several candidates: NK cells, CD4+ T cells, and CD8+ T cells in the spleen. The gating strategies for *ex vivo* stimulation with either phorbol 12-myristate 13-acetate (PMA)/ionomycin or CD3/CD28 purified antibodies, followed by extra- and intracellular staining, are illustrated in Supplementary Figure 2. We analyzed the immune cell profile of IFNAR1-/- and C57BL/6 mice infected with $7x10^5$ PFU D220 on day 5, 8, and 12 post infection. All data presented in Figure 5A-F are from a single infection.

First, we have repeatedly observed an enlarged spleen during the acute phase of infection in IFNAR1-/- mice compared to both resistant C57BL/6 mice and uninfected IFNAR1-/- mice. This finding is supported by the results of spleen-to-body-weight ratio and the number of splenocytes (Supplementary Figure 3), both of which are elevated in infected IFNAR1-/- mice. We speculated that this spleen enlargement may be due to the proliferation of immune cells when encountering viral infection; however, the increase in cell population could either be

generalized or limited to specific cell types. Therefore, we first sought to obtain an overview of the immune cells dynamics and assess their proportions before examining their absolute numbers.

During the peak of dengue morbidity (day 5 post infection), we observed a higher-than-baseline percentage of NK cells in the spleen of infected IFNAR1-/- mice, which act as the first line of defense against viral infection (Figure 5A). When the IFNAR1-/- mice recovered from infection and regained weight (day 8 and day 12 post infection), the adaptive immune response, notably T cells, became more prominent (Figure 5A). In our mouse model infected with D220, CD8+ T cells increased more than 10% in the infected IFNAR1-/- mice compared to uninfected IFNAR1-/- mice (Figure 5A). This corresponds to an increase of over 90 million CD8+ T cells compared to baseline levels (Figure 5B). In contrast, the immune cell profile of C57BL/6 resistant remained stable throughout the course of infection. However, the baseline for C57BL/6 mice should be re-evaluated using uninfected C57BL/6 mice to accurately assess infection-induced modulation of immune cell populations.

To investigate the IFNγ producers in D220 infection, we stimulated splenocytes with either PMA/ionomycin or CD3/CD28 and analyzed the intracellular production of IFNγ in parallel. PMA/ionomycin are strong activators of downstream T cell signaling pathways without the involvement of T cell receptor (TCR). Purified CD3/CD28 antibodies modulate naturally engage TCR signaling pathway. Under both stimulation methods, we have seen increased IFNγ production in infected IFNAR1-/- mice (16.1% IFNγ+ CD8 T cells for PMA/ionomycin, 6.0% IFNγ+ CD8 T cells for CD3/CD28) in contrast to C57BL/6 mice (3.5% IFNγ+ CD8 T cells for PMA/ionomycin, 1.3% IFNγ+ CD8 T cells for CD3/CD28). Uninfected IFNAR1-/- mice had 1.3% of IFNγ production when under PMA/ionomycin stimulation.

To take a step further, we speculated that DENV infection may alter the phenotype of CD8+ lymphocytes. We examined the effector/activated T cells with CD62L-/CD44+ markers.

Downregulation of CD62L (L-selectin) combined with upregulation of CD44 (H-CAM) allows the migration of T cells towards the site of infection. In Figure 5D, the CD8+ lymphocytes had shifted from CD62L+/CD44- naïve T cells in uninfected IFNAR1-/- mice to CD62L-/CD44+ effector T cell fate. Infected IFNAR1-/- mice had 82.5% CD8+ lymphocytes that were effector T cells compared to 11.6% in C57BL/6 wild-type controls, which are resistant to D220 infection (Figure 5F). Uninfected IFNAR1-/- mice had 5.8% effector T cells.

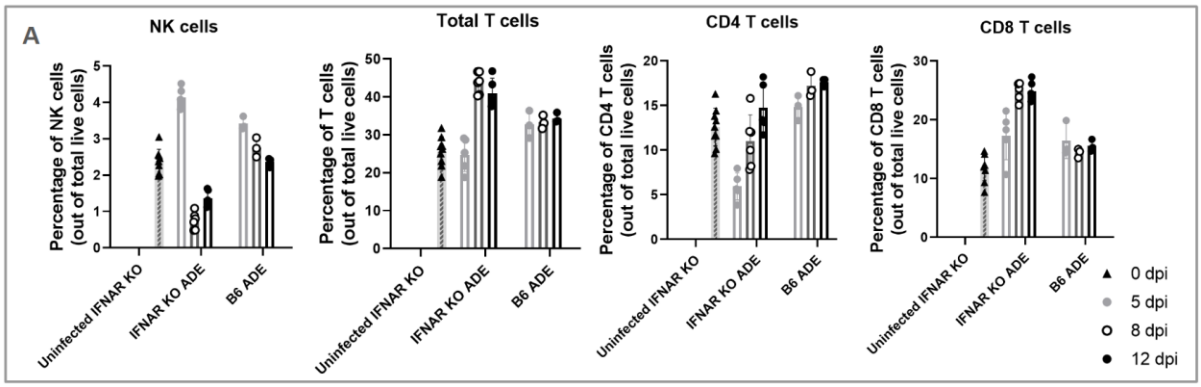
A
NK cells
Total T cells
CD4 T cells
CD8 T cells
Percentage of NK cells (out of total live cells)
Percentage of T cells (out of total live cells)
Percentage of CD4 T cells (out of total live cells)
Percentage of CD8 T cells (out of total live cells)
Uninfected IFNAR KO
IFNAR KO ADE
B6 ADE
0 dpi
5 dpi
8 dpi
12 dpi

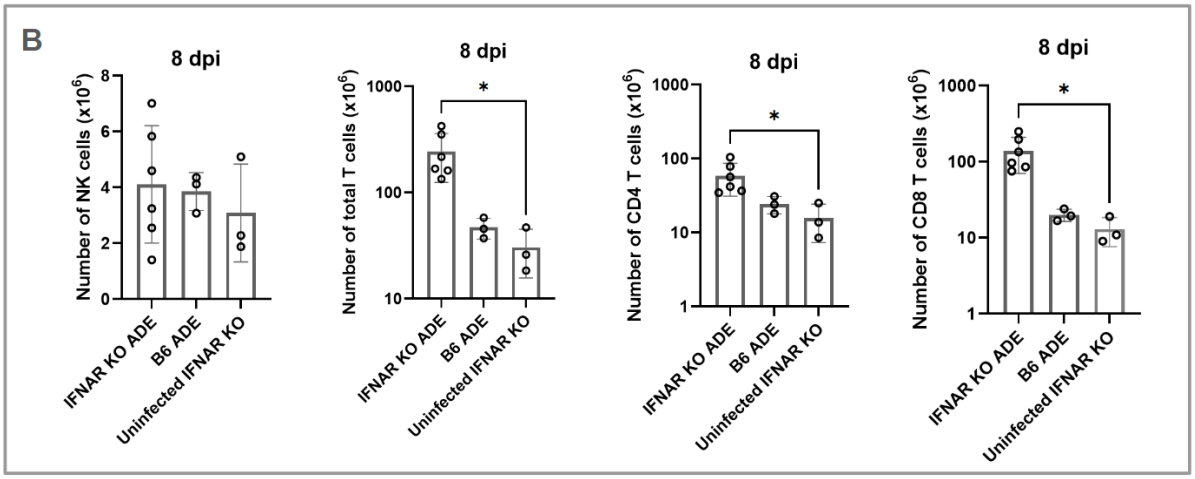
B
8 dpi
Number of NK cells (x10^6)
Number of total T cells (x10^6)
Number of CD4 T cells (x10^6)
Number of CD8 T cells (x10^6)
IFNAR KO ADE
B6 ADE
Uninfected IFNAR KO

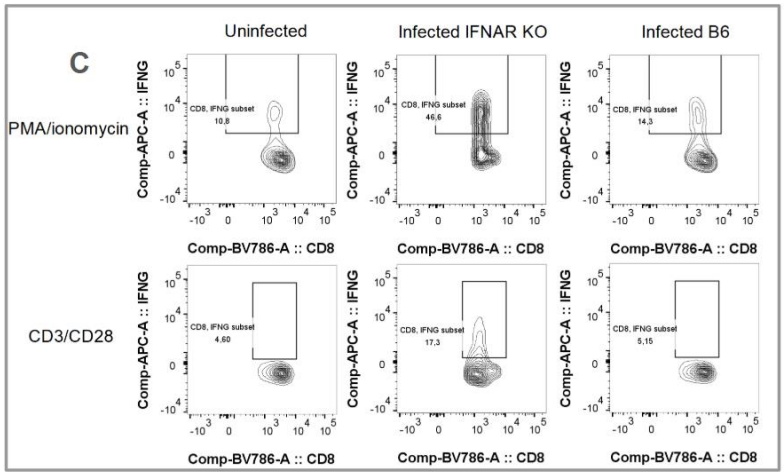
C
Uninfected
Infected IFNAR KO
Infected B6
PMA/ionomycin
CD3/CD28
Comp-APC-A :: IFNG
Comp-BV786-A :: CD8
CD8, IFNG subset
10,8
46,6
14,3
4,60
17,3
5,15

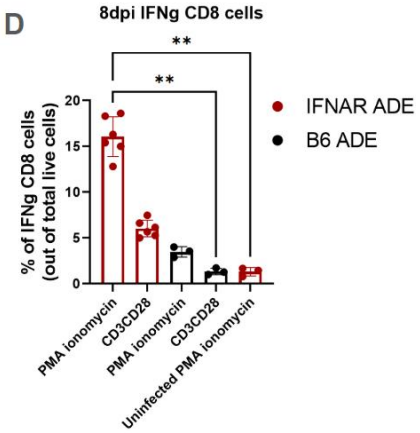
D
8dpi IFNg CD8 cells
% of IFNg CD8 cells (out of total live cells)
IFNAR ADE
B6 ADE
PMA ionomycin
CD3CD28
Uninfected PMA ionomycin

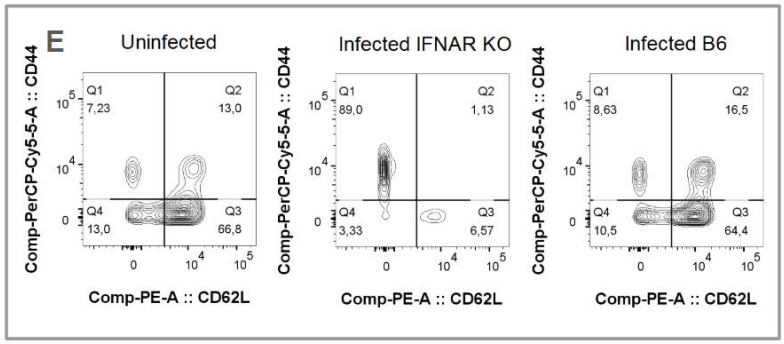
E
Uninfected
Infected IFNAR KO
Infected B6
Comp-PerCP-Cy5-5-A :: CD44
Comp-PE-A :: CD62L
Q1
Q2
Q3
Q4
7,23
13,0
13,0
66,8
89,0
1,13
3,33
6,57
8,63
16,5
10,5
64,4

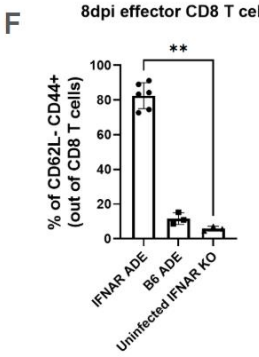
F
8dpi effector CD8 T cells
% of CD62L- CD44+ (out of CD8 T cells)
IFNAR ADE
B6 ADE
Uninfected IFNAR KO

Figure 5. Immune cell dynamics in IFNAR1-/- mice post D220 infection. Fluorescence minus one (FMO) controls for each color and isotype controls for IFNγ staining were included in every flow cytometry experiment (data not shown). Splenocytes were isolated by manually dissociating the tissue in Roswell Park Memorial Institute (RPMI) medium with 10% FBS, followed by treatment with 1 mL of RBC Lysing Buffer Hybri-Max **(A)** To establish baseline immune cell levels, uninfected IFNAR1-/- mice were sacrificed and splenocytes were isolated for evaluation. In addition, since immune cell dynamics were examined at day 5, 8, and 12 post infection, 3 uninfected IFNAR1-/- were sacrificed at each timepoint to account for variations in staining and acquisition performed across separate experiments. **(B)** The exact number of cells for each population was determined by normalizing the percentage of each population to the number of splenocytes derived from an entire spleen for each mouse. **(C-D)** FACS was performed for 1 million splenocytes stimulated *ex vivo* with PMA/ionomycin or CD3/CD28 purified antibodies, in combination with Brefeldin A and monensin for 4 hours at 37ºC. RPMI supplemented with 10% FBS was an unstimulated control. **(E-F)** CD62L+/CD44- naïve T cells in Q3 were defined as naïve T cells. CD62L-/CD44+ cells were defined as effector/activated T cells. p*<0.05, p**<0.01using Kruskal-Wallis test and Dunn's multiple comparison test.

Identification of DENV-specific CD8+ T cells Having established that the peak T cell response occurs around 8 days post infection, when we observed the highest IFNγ production from effector CD8+ T cell (Figure 5), we aimed to confirm the presence of DENV-specific CD8+ T cells in mice exposed to DENV. To achieve this, we stimulated splenocytes with DENV-specific peptides [64], in the presence of Brefeldin A to block the excretion of intracellular cytokines. We stimulated one million splenocytes *ex vivo* with a pool of DENV-specific peptides (C 51-59, NS4B 66-74, NS4B 99-107, 2 μg each, the exact sequences are indicated in Supplementary Table 4) and compared the response to a control ovalbumin (OVA) peptide.

In Figure 6A, we observed 16.2% of CD8+ T cells from infected IFNAR1-/- mice stimulated with DENV-specific peptides were capable of producing IFNγ, compared to less than 1% in uninfected IFNAR1-/- splenocytes stimulated with DENV-specific peptides. The Brefeldin A-only group served as a control for baseline IFNγ secretion without peptide stimulation and showed less than 1% IFNγ secretion. Stimulation with OVA peptide; however, resulted in comparable IFNγ detection in infected IFNAR1-/- splenocytes as stimulation with DENV-specific peptides. We observed infection-specific positive signal from both viral-

specific and control peptide and reasoned that e*x vivo* stimulation with peptides relies on the binding of these peptides to major histocompatibility complex (MHC) molecules on APCs, followed by their presentation to TCRs, which is not always efficient.

In an alternative approach, we utilized customized MHC tetramers from the NIH Tetramer Core Facility and tested the same 3 candidate peptides (C 51-59, NS4B 66-74, NS4B 99-107) and a negative control peptide (SARS-CoV-2 N 219-227). In this case, MHC molecules and the peptides form complexes and are linked to fluorochromes, so a signal detected by flow cytometry would indicate a cell recognizing this viral-specific peptide. In addition, MHC/peptide multimers can engage more than one copy of the TCR and increase the avidity of the test [93].

As shown in Figure 6B, 12.8% of CD8+ T cells from infected IFNAR1-/- mice were NS4B 99-107 positive, compared to less than 1% in uninfected IFNAR1-/- mice. The negative control marker showed less than 1% positive signal for both infected and uninfected splenocytes. Therefore, NS4B 99-107 serves as an indicator of DENV-experienced CD8+ T cells.

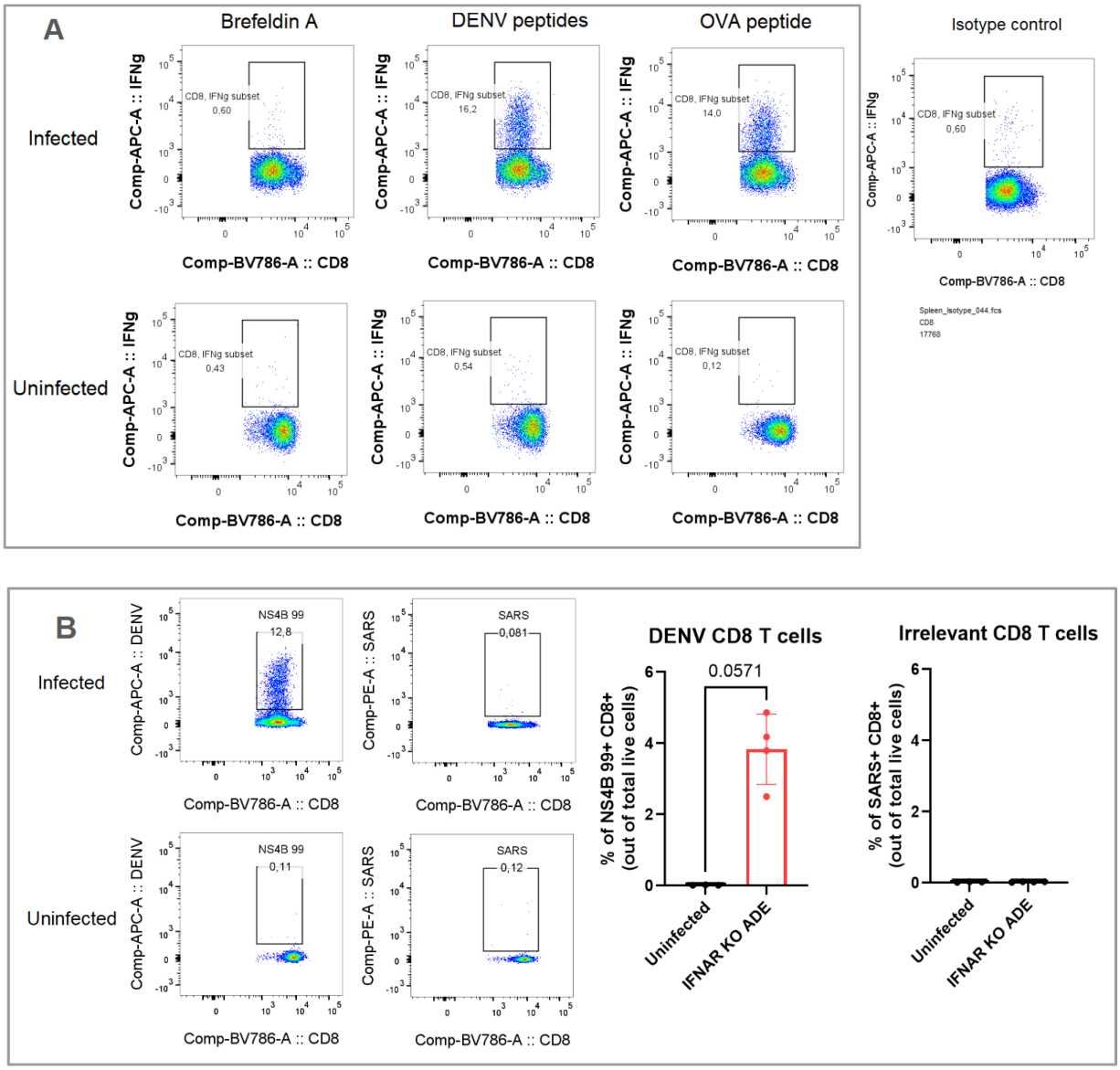

Figure 6 Identification of DENV-specific CD8+ T cells. All data presented in Figure 6 are from a single infection. Splenocytes were isolated by manually dissociating the tissue in RPMI medium with 10% FBS, followed by treatment with 1 mL of RBC Lysing Buffer Hybri-Max **(A)** An isotype control for IFNγ was included. The cells were gated as Live/dead negative, CD45 positive, TCRB positive, CD8 positive, CD4 negative, IFNγ positive. **(B)** Tetramer markers were stained in the same way as surface staining. P-value computed using Mann-Whitney test.

Chapter IV: discussion and limitations

Discussion

Our study aimed to develop a mouse model to investigate severe dengue infection and assess the potential for CD8+ T cell-targeting vaccine trials. The type I interferon receptor (IFNAR1) plays a crucial role in innate immune response against pathogens. Knocking out IFNAR1 renders our mouse model susceptible to the mouse-adapted D220 dengue 2 strain, resulting in body weight loss, increased mortality, elevated viral load in the circulation, and higher levels of proinflammatory cytokines IFN-γ, TNF-α, IL-6, and MCP-1. In contrast, immunocompetent C57BL/6 mice are resistant to D220 infection as they do not experience weight loss, nor succumb to infection, and demonstrate comparable levels of viral titer and inflammatory cytokine to uninfected IFNAR1-/-. These findings confirmed the susceptibility of IFNAR1-/- mice and the relevance of this model for studying dengue infection.

A key aspect of our investigation was exploring antibody dependent enhancement (ADE). Administering anti-flavivirus antibodies at sub-neutralizing levels results in higher mortality and morbidity in ADE IFNAR1-/- mice compared to infected IFNAR1-/- mice under non-ADE conditions. The main morbidity observed in these mice is reduced responsiveness to touch, characterized by inactivity and decreased mobility. To rule out the possibility that this was caused by the virus becoming neurotropic and affecting motor function, we plan to assess this further. Although less likely, if the virus crosses the blood-brain barrier and replicates in the brain, we might expect to observe paralysis in severe cases. Given that rare cases of dengue fever have been reported to affect the nervous system [94], we want to evaluate this potential. Therefore, we can estimate the viral titer in the brain using qPCR.

Even though the penetrance of dengue virus increases under ADE conditions, no significant difference in viral load or in inflammatory cytokines levels was observed between ADE and non-ADE IFNAR1-/- mice infected with D220. Assessing the degree of vascular

leakage in organs such as the intestine, spleen, and liver, which have demonstrated increased vascular permeability in our severe dengue IFNAR1-/- model, could provide insight into the difference between ADE and non-ADE conditions. Investigating the levels of NS1 viral protein, which correlates with endothelial permeability in a dose-dependent manner *in vitro* [95], rather than focusing solely on mRNA viral transcripts for viral load could be a promising avenue to understand the mechanisms behind severe dengue manifestation driven by ADE. However, studies in human patients with severe dengue gave controversial results, revealing discordance in the timing of vascular leakage and NS1 antigenemia which could depend on the serotype of DENV [96].

Additionally, since blood in tissues cannot be completely removed even with perfusion, we cannot be entirely certain whether the virus is replicating in the tissue or simply present in the circulation based solely on viral transcripts from tissue homogenates. To address this, we plan to conduct fluorescence microscopy using viral-specific markers on tissue sections. This would allow us to directly visualize the presence of the virus within the tissue. An added benefit of this approach is that we can compare the pathology of infected versus uninfected tissue. For example, we can assess whether there is increased necrosis, inflammation, or immune cell infiltration in infected mice, which could be driven by elevated cytokine levels. Furthermore, in mice with more permeable tissues, it would be valuable to examine whether the tissue architecture has been altered.

The proinflammatory cytokines, which play a key role in triggering immune response, may act as a double-edge sword. For instance, a trend towards elevated blood levels of TNFα were detected during the acute phase of infection in IFNAR1-/- mice. The same cytokine may not only drive inflammation in the body but could also lead to adverse endothelial dysfunction and increased vascular permeability in mice. Therefore, studying the innate immune cells, such as macrophages and dendritic cells, that are targets of DENV infection and are known to secret

these cytokines during the acute phase of infection, could provide insight into the vascular leakage taking place during this period. CD8+ lymphocytes are also capable of secreting these proinflammatory cytokines; however, the timing of their emergence correlates with the recovery from non-lethal severe dengue disease, suggesting that CD8+ lymphocytes may play a more protective role against dengue than innate immune cells.

As part of our study's goal, we have described elevated levels of CD8+ T cells in IFNAR1-/- mice in response to dengue infection. The emergence of IFNγ-producing CD8+ T cells and the shift in lymphocyte phenotype from naïve to effector/activated CD8+ T cells indicate a robust antiviral immune response in DENV-infected IFNAR1-/- mice. Furthermore, DENV-specific CD8+ T cells were identified using the NS4B 99-107 tetramer. These findings suggest that our approach to characterize the CD8+ T cell phenotype in response to dengue infection is effective. However, since the immune response depends on interactions among various cell types, we speculate that other antiviral cells, such as CD4+ Th1 cells, may also be involved in combating viral infection. Moreover, evaluating a subset of CD8+ T cells known as Tc1 cells, which are particularly recognized for their cytotoxicity activity, in greater detail could provide further insight beyond evaluating CD8+ T cells in general.

To further characterize the cytotoxicity of CD8+ T cells, we propose using a more specific panel. This panel would not only detect antiviral cytokines such as IFNγ and TNFα but also include degranulation markers like CD107a, as well as the enzymes perforin and granzyme B that disrupt the integrity of cell membrane and lead to elimination of infected cells. After establishing how CD8+ T cells expand and function during infection, we can move on to investigate the phase when antigens are cleared. Exhaustion markers such as PD-1 may indicate the waning of these effector T cells. However, we expect memory CD8+ T cells to persist and mount a robust response when re-encountering the dengue virus. This will be a key aspect of evaluating the efficacy of CD8+ T cell-targeting vaccines.

Limitations

One of the biggest challenges in animal studies is determining how applicable the findings are to human research. While several mouse models have been developed for dengue research, each with specific strengths and weaknesses, we chose to use IFNAR1-/- mice combined with a mouse-adapted dengue virus to induce severe dengue without completely disrupting the immune response. This choice reflects the need to balance model relevance with the ability to generate severe disease symptoms similar to those seen in human cases.

The D220 viral strain used in this study contains several amino acid mutations distinct from its parental strain, PL046, which originated from a human DENV2 clinical isolate. D220 infection leads to higher mortality and morbidity in IFNAR1-/- mice compared to the PL046 strain [83] and contains five missense mutations compared to PL046: I106F in the capsid protein, K122I and N124D in the envelope protein, S228P in the NS1 protein, and V115A in the NS4B protein [83]. We conducted Sanger sequencing (data not shown) to confirm that our D220 stock contains the same point mutations as previously reported. Despite these confirmations, further investigation is needed to understand the clinical relevance of D220 infections in mice to human dengue disease. Such research is critical for translating findings from this model to human dengue infections and will help determine whether D220 accurately reflects the pathogenesis of severe dengue in humans.

Another concern with this model is the unclear role of type I interferon signaling in the CD8+ T cell response during dengue infection. Previous studies have shown that the absence of type I interferon receptors in CD8+ T cells impair their clonal expansion during lymphocytic choriomeningitis virus (LCMV) infection [97]. This raises questions about the validity of our model, as IFNAR1-/- mice may not fully mimic the immune dynamics observed in humans. However, our D220 infection model using global type I interferon receptor knockout mice displayed a robust primary clonal expansion of DENV-specific effector CD8+ T cells. This

suggests that other cytokines, such as IL-12, may compensate for the absence of type I interferon signals, as has been reported in vaccinia viral infection [98]. Further research is required to assess whether the type I interferon receptor knockout influences the long-term development of memory CD8+ T cells and whether the effector functions of these cells are compromised. These studies will help clarify the utility of our model in studying CD8+ T cell-mediated immunity and vaccine responses.

Although the use of an immunodeficient mouse model, such as IFNAR1-/-, may limit our ability to fully characterize intact immune responses post infection or vaccination, there are ways to address this limitation. One approach is to vaccinate immunocompetent C57BL/6 mice and then transfer CD8+ T cells into the immunodeficient model. This method allows us to indirectly assess the efficacy of CD8+ T cell targeting vaccines in conferring protection against dengue. By evaluating key outcomes such as reduced mortality, morbidity, and viral load in the immunodeficient mice following T cell transfer, we can gain valuable insights into the potential protective effects of the vaccine. This strategy aligns with the overarching goal of the project, which is to develop a mouse model that helps in evaluating vaccines capable of providing protection against severe dengue infection.

Lastly, a common limitation of all animal studies is the sample size and the replicability of results. To address this, we carefully selected doses for the viral inoculum to ensure consistency in survival rates and disease severity post infection. While we have included both male and female mice in our experiments and have not observed any significant sex differences so far, further studies are needed to confirm these findings across all relevant parameters. Moreover, we plan to explore potential age-related variations in future trials to rule out subtle effects that may influence disease progression or immune responses. By investigating these variables, we aim to strengthen the reliability and translational potential of our model for studying severe dengue.

Chapter V: future directions and conclusion

Future Directions

We crossed the IFNAR1 knockout mice with a CD8+ T cell knockout strain obtained from the Jackson Library (CD8-/-: B6.129S2-Cd8a^{tm1Mak}/J strain number 002665) [89] to generate double knockout mice deficient in both the type I interferon receptor and functional CD8+ T cells. This model will allow us to evaluate how the absence of CD8+ T cells impacts the clinical outcomes of dengue infection and assess the protective role that CD8+ lymphocytes may play during the recovery phase. The key parameters we plan to assess include: 1) survival, clinical score, vascular permeability, and percentage of body weight loss upon challenge 2) viral load and proinflammatory cytokines post infection; and 3) the presence of dengue-specific cytotoxic CD8+ T cells. By understanding the responses of CD8/IFNAR1 double knockout mice to dengue infection, we can then proceed with CD8+ T cell transfer experiments from DENV-NS poly-epitope vaccinated mice into the double knockout model.

In addition, we can explore crossing IFNAR1-/- mice with strains deficient in other immune cell types, such as mature B cells, to investigate the role of B cells and antibodies in the dengue immune response. We are also considering the use of alternative dengue-susceptible mouse models, including human STAT2 knock-in mice. This model has been established for studying Zika viral infection and may also be suitable for dengue, as both viruses evade the immune response in human by degrading STAT2 protein through its NS5 protein [99]. The human STAT2 knock-in mice would serve as an immunocompetent model, providing greater relevance to human dengue infections. Advancing this model and evaluating the potential to induce severe dengue would be an interesting project. These future directions aim to enhance our understanding of the immune mechanisms involved in dengue infection and evaluate potential therapeutic strategies.

Conclusion

Laboratory mice comprising an expeditious model for preclinical vaccine testing and the identification of correlates of vaccine protection. We have built a mouse model susceptible to DENV infection, which also recapitulates features of severe dengue disease under ADE. D220 infection triggered a robust antiviral response, particularly seen in IFNγ secreting CD8+ T cells. Although the inherent limitations of immunodeficient models necessitate careful interpretation, our strategy of CD8+ T cell transfer from immunocompetent mice holds promise for overcoming these challenges. Our research aims to better replicate human dengue symptoms and facilitate the translation of preclinical findings to clinical applications. Ultimately, our goal is to contribute to the development of more effective dengue vaccines and therapeutic strategies.

Chapter VI: references

1. Horstick, O., Y. Tozan, and A. Wilder-Smith, *Reviewing dengue: still a neglected tropical disease?* PLoS Negl Trop Dis, 2015. **9**(4): p. e0003632.
2. Bhatt, S., et al., *The global distribution and burden of dengue.* Nature, 2013. **496**(7446): p. 504-7.
3. Roy, S.K. and S. Bhattacharjee, *Dengue virus: epidemiology, biology, and disease aetiology.* Can J Microbiol, 2021. **67**(10): p. 687-702.
4. Guzman, M.G., M. Alvarez, and S.B. Halstead, *Secondary infection as a risk factor for dengue hemorrhagic fever/dengue shock syndrome: an historical perspective and role of antibody-dependent enhancement of infection.* Arch Virol, 2013. **158**(7): p. 1445-59.
5. Sawant, J., A. Patil, and S. Kurle, *A Review: Understanding Molecular Mechanisms of Antibody-Dependent Enhancement in Viral Infections.* Vaccines (Basel), 2023. **11**(7).
6. Sridhar, S., et al., *Effect of Dengue Serostatus on Dengue Vaccine Safety and Efficacy.* N Engl J Med, 2018. **379**(4): p. 327-340.
7. Weiskopf, D., et al., *Comprehensive analysis of dengue virus-specific responses supports an HLA-linked protective role for CD8+ T cells.* Proc Natl Acad Sci USA, 2013. **110**(22): p. E2046-53.
8. Roth, C., et al., *A Modified mRNA Vaccine Targeting Immunodominant NS Epitopes Protects Against Dengue Virus Infection in HLA Class I Transgenic Mice.* Frontiers in Immunology, 2019. **10**.
9. Philippe Buchy, C.R., Anavaj Sakuntabhai, Etienne Simon-Loriere, Frederic Tangy, *A dengue virus chimeric polyepitope composed of fragments of non-structural proteins and its use in an immunogenic composition against dengue virus infection*, WO2015197565A1, E.P. Office, Editor. Dec 30, 2015.
10. PDN, N.S., et al., *Concurrent dengue infections: Epidemiology & clinical implications.* Indian J Med Res, 2021. **154**(5): p. 669-679.
11. Wang, E., et al., *Evolutionary relationships of endemic/epidemic and sylvatic dengue viruses.* J Virol, 2000. **74**(7): p. 3227-34.
12. Messina, J.P., et al., *Global spread of dengue virus types: mapping the 70 year history.* Trends Microbiol, 2014. **22**(3): p. 138-46.
13. Nakase, T., et al., *Population at risk of dengue virus transmission has increased due to coupled climate factors and population growth.* Communications Earth & Environment, 2024. **5**(1): p. 475.
14. Childs, M. L., et al. (2024). *Climate warming is expanding dengue burden in the Americas and Asia.* medRxiv : 2024.01.08.24301015.
15. Kolimenakis, A., et al., *The role of urbanisation in the spread of Aedes mosquitoes and the diseases they transmit-A systematic review.* PLoS Negl Trop Dis, 2021. **15**(9): p. e0009631.

16. Colón-González, F.J., et al., *Projecting the risk of mosquito-borne diseases in a warmer and more populated world: a multi-model, multi-scenario intercomparison modelling study.* Lancet Planet Health, 2021. **5**(7): p. e404-e414.
17. Lozano-Fuentes, S., et al., *The dengue virus mosquito vector Aedes aegypti at high elevation in Mexico.* Am J Trop Med Hyg, 2012. **87**(5): p. 902-9.
18. Brady, O.J. and S.I. Hay, *The Global Expansion of Dengue: How Aedes aegypti Mosquitoes Enabled the First Pandemic Arbovirus.* Annu Rev Entomol, 2020. **65**: p. 191-208.
19. Guzman, M.G., et al., *Dengue infection.* Nat Rev Dis Primers, 2016. **2**(1): p. 16055.
20. Chan, M. and M.A. Johansson, *The Incubation Periods of Dengue Viruses.* PLOS ONE, 2012. **7**(11): p. e50972.
21. Christofferson, R.C. and C.N. Mores, *Potential for Extrinsic Incubation Temperature to Alter Interplay Between Transmission Potential and Mortality of Dengue-Infected Aedes aegypti.* Environ Health Insights, 2016. **10**: p. 119-23.
22. Watts, D.M., et al., *Effect of temperature on the vector efficiency of Aedes aegypti for dengue 2 virus.* Am J Trop Med Hyg, 1987. **36**(1): p. 143-52.
23. Pan American Health Organization. *Reported Cases of Dengue Fever in The Americas.* July 07. 2024, https://www3.paho.org/data/index.php/en/mnu-topics/indicadores-dengue-en/dengue-nacional-en/252-dengue-pais-ano-en.html.
24. Public Health Agency of Canada. *"Dengue Fever." Canada.ca*, 13 Aug. 2024, www.canada.ca/en/public-health/services/infectious-diseases/viral-haemorrhagic-fevers/dengue-fever/surveillance.html.
25. TravelWeek. *Caribbean welcomes strong performance from Canada.* http://www.travelweek.ca/news/caribbean-welcomes-strong-performance-from canada-up-5-7-with-3-9-million-visits-in-2018/ (2018).
26. TravelWeek. *Record year for Cuba especially from this market; Canada is Cuba's "top priority"*. https://www.travelweek.ca/news/record-year-cuba-especially-market-canada cubas-top-priority/ (2017).
27. Canada, Global Affairs. *"Canada-Mexico Relations." GAC*, May 10. 2024, www.international.gc.ca/country-pays/mexico-mexique/relations.aspx?lang=eng
28. Khan, S.U., et al., *Current and Projected Distributions of Aedes aegypti and Ae. albopictus in Canada and the U.S.* Environ Health Perspect, 2020. **128**(5): p. 57007.
29. van Leur, S.W., et al., *Pathogenesis and virulence of flavivirus infections.* Virulence, 2021. **12**(1): p. 2814-2838.
30. Rana, J., et al., *Dengue virus capsid anchor modulates the efficiency of polyprotein processing and assembly of viral particles.* J Gen Virol, 2019. **100**(12): p. 1663-1673.
31. Li, Q. and C. Kang, *Structures and Dynamics of Dengue Virus Nonstructural*

Membrane Proteins. Membranes (Basel), 2022. **12**(2).
32. Perera-Lecoin, M., et al., *Flavivirus entry receptors: an update.* Viruses, 2013. **6**(1): p. 69-88.
33. Byk, L.A. and A.V. Gamarnik, *Properties and Functions of the Dengue Virus Capsid Protein.* Annu Rev Virol, 2016. **3**(1): p. 263-281.
34. Rodenhuis-Zybert, I.A., J. Wilschut, and J.M. Smit, *Dengue virus life cycle: viral and host factors modulating infectivity.* Cell Mol Life Sci, 2010. **67**(16): p. 2773-2786.
35. Sinha, S., et al., *Dengue virus pathogenesis and host molecular machineries.* Journal of Biomedical Science, 2024. **31**(1): p. 43.
36. Modis, Y., et al., *Structure of the dengue virus envelope protein after membrane fusion.* Nature, 2004. **427**(6972): p. 313-9.
37. Clyde, K., J.L. Kyle, and E. Harris, *Recent advances in deciphering viral and host determinants of dengue virus replication and pathogenesis.* J Virol, 2006. **80**(23): p. 11418-31.
38. Falgout, B., et al., *Both nonstructural proteins NS2B and NS3 are required for the proteolytic processing of dengue virus nonstructural proteins.* J Virol, 1991. **65**(5): p. 2467-75.
39. Nomaguchi, M., et al., *De novo synthesis of negative-strand RNA by Dengue virus RNA-dependent RNA polymerase in vitro: nucleotide, primer, and template parameters.* J Virol, 2003. **77**(16): p. 8831-42.
40. Mukhopadhyay, S., R.J. Kuhn, and M.G. Rossmann, *A structural perspective of the flavivirus life cycle.* Nat Rev Microbiol, 2005. **3**(1): p. 13-22.
41. Gutsche, I., et al., *Secreted dengue virus nonstructural protein NS1 is an atypical barrel-shaped high-density lipoprotein.* Proc Natl Acad Sci USA, 2011. **108**(19): p. 8003-8008.
42. Modhiran, N., et al., *Dengue virus NS1 protein activates cells via Toll-like receptor 4 and disrupts endothelial cell monolayer integrity*. Sci Transl Med, 2015. **7**(304): p. 304ra142-304ra142.
43. Seynhaeve, A.L., et al., *Exposing endothelial cells to tumor necrosis factor-α and peripheral blood mononuclear cells damage endothelial integrity via interleukin-1ß by degradation of vascular endothelial-cadherin.* Surgery, 2014. **155**(3): p. 545-53.
44. Lee, Y.R., et al., *MCP-1, a highly expressed chemokine in dengue haemorrhagic fever/dengue shock syndrome patients, may cause permeability change, possibly through reduced tight junctions of vascular endothelium cells.* J Gen Virol, 2006. **87**(Pt 12): p. 3623-3630.
45. Chen, H.R., et al., *Macrophage migration inhibitory factor is critical for dengue NS1-induced endothelial glycocalyx degradation and hyperpermeability.* PLoS Pathog, 2018. **14**(4): p. e1007033.

46. Kularatne, S.A. and C. Dalugama, *Dengue infection: Global importance, immunopathology and management.* Clin Med (Lond), 2022. **22**(1): p. 9-13.
47. Katzelnick, L.C., et al., *Antibody-dependent enhancement of severe dengue disease in humans.* Science, 2017. **358**(6365): p. 929-932.
48. World Health Organization. (1997). *Dengue haemorrhagic fever : diagnosis, treatment, prevention and control, 2nd ed.* World Health Organization. Geneva, https://iris.who.int/handle/10665/41988
49. Rothman, A.L., *Dengue: defining protective versus pathologic immunity.* J Clin Invest, 2004. **113**(7): p. 946-951.
50. World Health Organization. (2009). *Dengue guidelines for diagnosis, treatment, prevention and control : new edition.* World Health Organization. Geneva, https://iris.who.int/handle/10665/44188
51. Bournazos, S., et al., *Antibody fucosylation predicts disease severity in secondary dengue infection.* Science, 2021. **372**(6546): p. 1102-1105.
52. Wang, T.T., et al., *IgG antibodies to dengue enhanced for FcγRIIIA binding determine disease severity.* Science, 2017. **355**(6323): p. 395-398.
53. Halstead, S.B., et al., *Dengue hemorrhagic fever in infants: research opportunities ignored.* Emerg Infect Dis, 2002. **8**(12): p. 1474-9.
54. Simmons, C.P., et al., *Maternal antibody and viral factors in the pathogenesis of dengue virus in infants.* J Infect Dis, 2007. **196**(3): p. 416-24.
55. Ng, J.K., et al., *First experimental in vivo model of enhanced dengue disease severity through maternally acquired heterotypic dengue antibodies.* PLoS Pathog, 2014. **10**(4): p. e1004031.
56. Nasirudeen, A.M., et al., *RIG-I, MDA5 and TLR3 synergistically play an important role in restriction of dengue virus infection.* PLoS Negl Trop Dis, 2011. **5**(1): p. e926.
57. Ho, L.J., et al., *Infection of human dendritic cells by dengue virus causes cell maturation and cytokine production.* J Immunol, 2001. **166**(3): p. 1499-506.
58. Shelburne, C.P., et al., *Mast cells augment adaptive immunity by orchestrating dendritic cell trafficking through infected tissues.* Cell Host Microbe, 2009. **6**(4): p. 331-42.
59. Haller, O., G. Kochs, and F. Weber, *The interferon response circuit: induction and suppression by pathogenic viruses.* Virology, 2006. **344**(1): p. 119-30.
60. St. John, A.L. and A.P.S. Rathore, *Adaptive immune responses to primary and secondary dengue virus infections.* Nat Rev Immunol, 2019. **19**(4): p. 218-230.
61. Lindow, J.C., et al., *Primary vaccination with low dose live dengue 1 virus generates a proinflammatory, multifunctional T cell response in humans.* PLoS Negl Trop Dis, 2012. **6**(7): p. e1742.
62. Tian, Y., et al., *Human T Cell Response to Dengue Virus Infection.* Front Immunol, 2019. **10**: p. 2125.

63. Friberg, H., et al., *Cross-reactivity and expansion of dengue-specific T cells during acute primary and secondary infections in humans.* Sci Rep, 2011. **1**: p. 51.
64. Yauch, L.E., et al., *A protective role for dengue virus-specific CD8+ T cells.* J Immunol, 2009. **182**(8): p. 4865-73.
65. Vatti, A., et al., *Original antigenic sin: A comprehensive review.* J Autoimmun, 2017. **83**: p. 12-21.
66. Wang, W.H., et al., *Targets and strategies for vaccine development against dengue viruses.* Biomed Pharmacother, 2021. **144**: p. 112304.
67. Prompetchara, E., et al., *Dengue vaccine: Global development update.* Asian Pac J Allergy Immunol, 2020. **38**(3): p. 178-185.
68. Biswal, S., et al., *Efficacy of a Tetravalent Dengue Vaccine in Healthy Children and Adolescents.* N Engl J Med, 2019. **381**(21): p. 2009-2019.
69. Tricou, V., et al., *Safety and immunogenicity of a tetravalent dengue vaccine in children aged 2-17 years: a randomised, placebo-controlled, phase 2 trial.* Lancet, 2020. **395**(10234): p. 1434-1443.
70. Biswal, S., et al., *Efficacy of a tetravalent dengue vaccine in healthy children aged 4-16 years: a randomised, placebo-controlled, phase 3 trial.* Lancet, 2020. **395**(10234): p. 1423-1433.
71. Chan, K.W.K., et al., *Animal models for studying dengue pathogenesis and therapy.* Antiviral Research, 2015. **123**: p. 5-14.
72. Scherer, W.F., et al., *Experimental infection of chimpanzees with dengue viruses.* Am J Trop Med Hyg, 1978. **27**(3): p. 590-9.
73. Omatsu, T., et al., *Common marmoset (Callithrix jacchus) as a primate model of dengue virus infection: development of high levels of viraemia and demonstration of protective immunity.* J Gen Virol, 2011. **92**(Pt 10): p. 2272-2280.
74. Chen, R.E. and M.S. Diamond, *Dengue mouse models for evaluating pathogenesis and countermeasures.* Curr Opin Virol, 2020. **43**: p. 50-58.
75. Ashour, J., et al., *Mouse STAT2 restricts early dengue virus replication.* Cell Host Microbe, 2010. **8**(5): p. 410-21.
76. Aguirre, S., et al., *DENV inhibits type I IFN production in infected cells by cleaving human STING.* PLoS Pathog, 2012. **8**(10): p. e1002934.
77. Johnson, A.J. and J.T. Roehrig, *New mouse model for dengue virus vaccine testing.* J Virol, 1999. **73**(1): p. 783-6.
78. de Oliveira, L.C., et al., *The small molecule AZD6244 inhibits dengue virus replication in vitro and protects against lethal challenge in a mouse model.* Arch Virol, 2020. **165**(3): p. 671-681.
79. Milligan, G.N., et al., *Spectrum of activity testing for therapeutics against all four dengue virus serotypes in AG129 mouse models: Proof-of-concept studies with the*

adenosine nucleoside inhibitor NITD-008. Antiviral Res, 2018. **154**: p. 104-109.
80. Zellweger, R.M., T.R. Prestwood, and S. Shresta, *Enhanced infection of liver sinusoidal endothelial cells in a mouse model of antibody-induced severe dengue disease.* Cell Host Microbe, 2010. **7**(2): p. 128-39.
81. Elong Ngono, A., et al., *Protective Role of Cross-Reactive CD8 T Cells Against Dengue Virus Infection.* EBioMedicine, 2016. **13**: p. 284-293.
82. Müller, U., et al., *Functional role of type I and type II interferons in antiviral defense.* Science, 1994. **264**(5167): p. 1918-21.
83. Orozco, S., et al., *Characterization of a model of lethal dengue virus 2 infection in C57BL/6 mice deficient in the alpha/beta interferon receptor.* J Gen Virol, 2012. **93**(Pt 10): p. 2152-2157.
84. Espinosa, D.A., et al., *Cyclic Dinucleotide-Adjuvanted Dengue Virus Nonstructural Protein 1 Induces Protective Antibody and T Cell Responses.* J Immunol, 2019. **202**(4): p. 1153-1162.
85. Espinosa, D.A., et al., *Increased serum sialic acid is associated with morbidity and mortality in a murine model of dengue disease.* J Gen Virol, 2019. **100**(11): p. 1515-1522.
86. Pinto, A.K., et al., *Defining New Therapeutics Using a More Immunocompetent Mouse Model of Antibody-Enhanced Dengue Virus Infection.* mBio, 2015. **6**(5): p. e01316-15.
87. Janeway CA Jr, T.P., Walport M, et al., *T cell-mediated cytotoxicity*, in *Immunobiology: The Immune System in Health and Disease. 5th edition*. 2001: New York: Garland Science.
88. Lin, Y.L., et al., *Study of Dengue virus infection in SCID mice engrafted with human K562 cells.* J Virol, 1998. **72**(12): p. 9729-37.
89. Fung-Leung, W.-P., et al., *CD8 is needed for development of cytotoxic T but not helper T cells.* Cell, 1991. **65**(3): p. 443-449.
90. Case, J.B., et al., *Growth, detection, quantification, and inactivation of SARS-CoV-2.* Virology, 2020. **548**: p. 39-48.
91. Martina, B.E., P. Koraka, and A.D. Osterhaus, *Dengue virus pathogenesis: an integrated view.* Clin Microbiol Rev, 2009. **22**(4): p. 564-81.
92. Bhatt, P., et al., *Current Understanding of the Pathogenesis of Dengue Virus Infection.* Curr Microbiol, 2021. **78**(1): p. 17-32.
93. *Why Tetramers?, NIH Tetramer Core Facility*. Available from: https://tetramer.yerkes.emory.edu/tetramer-science/why-tetramers.
94. Trivedi, S. and A. Chakravarty, *Neurological Complications of Dengue Fever.* Curr Neurol Neurosci Rep, 2022. **22**(8): p. 515-529.
95. Beatty, P.R., et al., *Dengue virus NS1 triggers endothelial permeability and vascular leak that is prevented by NS1 vaccination.* Sci Transl Med, 2015. **7**(304): p. 304ra141-

304ra141.
96. Malavige, G.N. and G.S. Ogg, *Pathogenesis of vascular leak in dengue virus infection.* Immunology, 2017. **151**(3): p. 261-269.
97. Aichele, P., et al., *CD8 T cells specific for lymphocytic choriomeningitis virus require type I IFN receptor for clonal expansion.* J Immunol, 2006. **176**(8): p. 4525-9.
98. Xiao, Z., et al., *Programming for CD8 T cell memory development requires IL-12 or type I IFN.* J Immunol, 2009. **182**(5): p. 2786-94.
99. Gorman, M.J., et al., *An Immunocompetent Mouse Model of Zika Virus Infection.* Cell Host Microbe, 2018. **23**(5): p. 672-685.e6.
100. Israelow, B., et al., *Adaptive immune determinants of viral clearance and protection in mouse models of SARS-CoV-2.* Sci Immunol, 2021. **6**(64): p. eabl4509.

Appendix

Supplementary Figures

Supplementary Table 1. Scoring standards for morbidity. The parameters were adapted from [95], which also uses IFNAR1-/- mice and the same DENV D220 strain.

1	Healthy
2	Ruffled fur and mild signs of lethargy
3	Hunched posture, ruffled fur, and intermediate level of lethargy and failure to groom
4	Very lethargic, limited mobility, ruffled fur, and hunched posture
5	Found dead; Moribund with limited to no mobility and inability to reach food or water

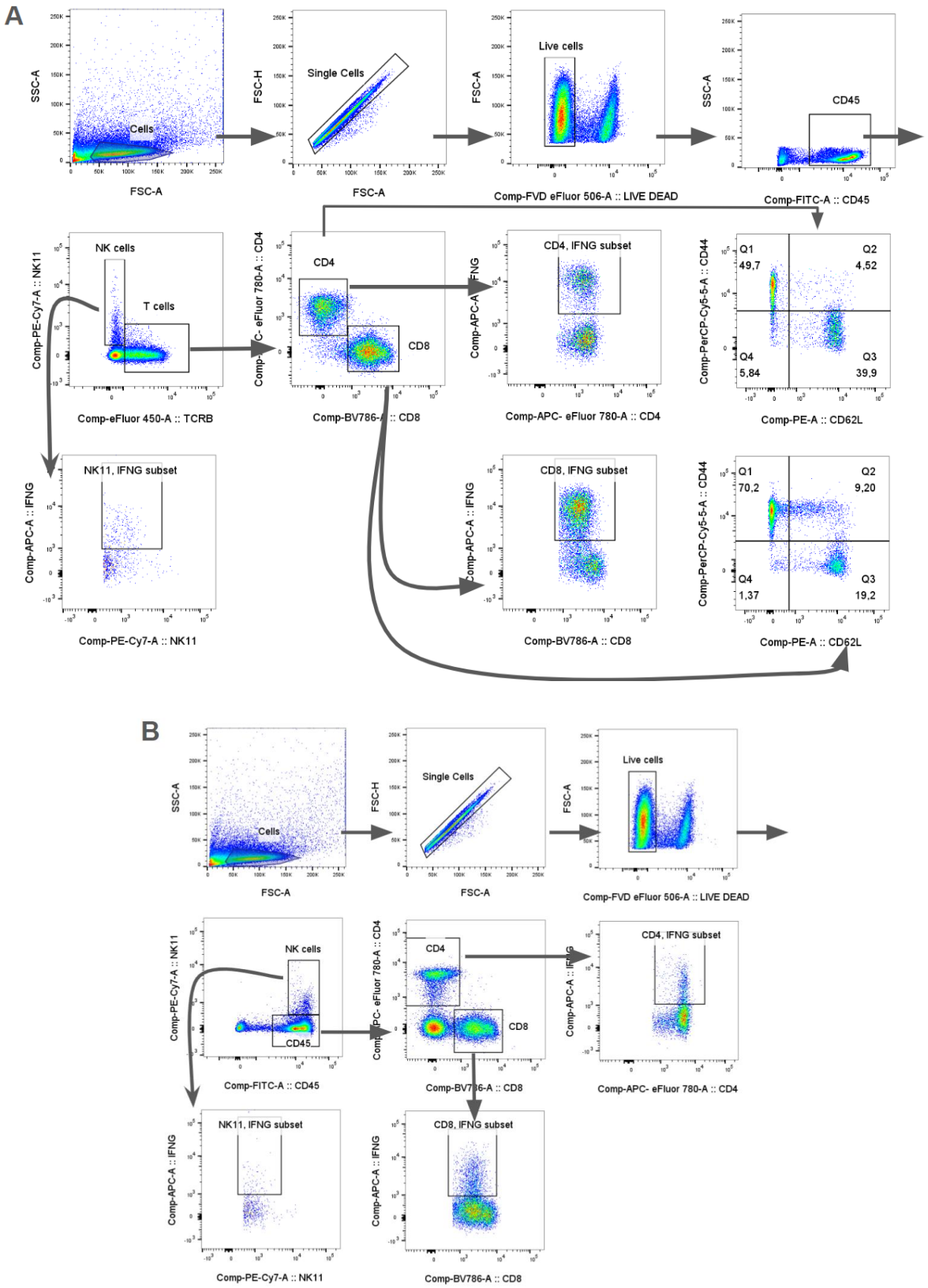

Supplementary Figure 2. Gating strategy for flow cytometry. (A) PMA/ionomycin stimulation or unstimulated splenocytes. **(B)** CD3/CD28 stimulation when TCR were engaged by these purified antibodies and thus the TCRB staining was not useful for distinguishing T cell populations.

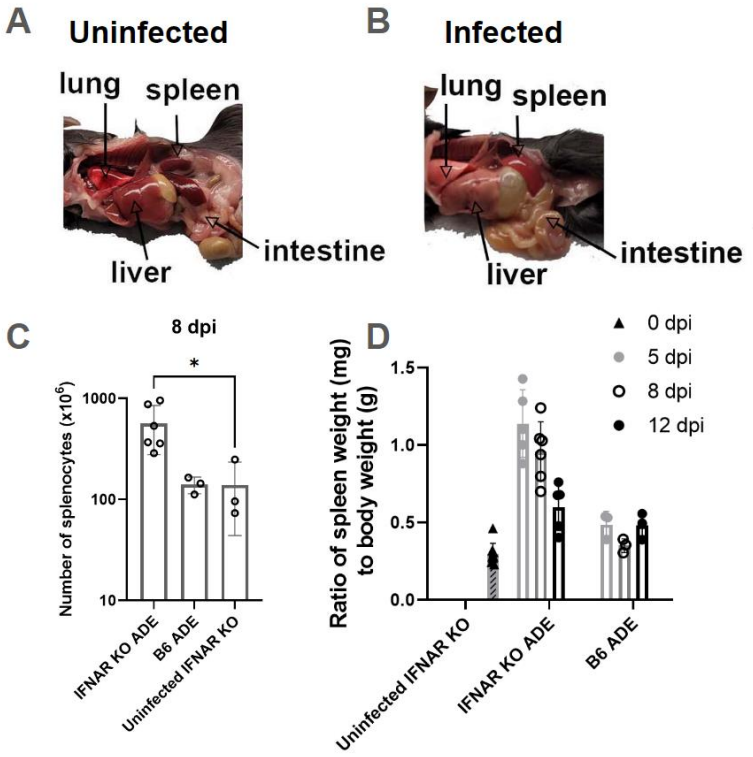

Supplementary Figure 3. Pictures taken during necropsy and the analysis of enlarged spleen. (A and B) Pictures of uninfected and infected mice were taken on day 5 post infection. Spleen and liver were pale and enlarged in infected mice compared to uninfected IFNAR1-/-. **(C)** The increase in the number of splenocytes for infected IFNAR1-/- was observed, while B6 ADE and uninfected IFNAR1-/- had comparable number of splenocytes. **(D)** Spleen weight of each mouse was divided by their body weight on day 0 post infection.

Supplementary Table 4. Peptide sequences for ex vivo stimulation and customized tetramers [64, 100].

Epitope	Sequence
C 51-59	VAFLRFLTI
NS4B 66-74	TAIANQATV
NS4B 99-107	YSQVNPITL
OVA 257-264	SIINFEKL
SARS-CoV-2 N 219-227	LALLLLDRL